Plasmodium P36 determines host cell receptor usage during sporozoite invasion

Giulia Manzoni[1], Carine Marinach[1*], Selma Topçu[1*], Sylvie Briquet[1], Morgane Grand[1], Matthieu Tolle[1], Marion Gransagne[1], Julien Lescar[1], Chiara Andolina[2,3], Jean-François Franetich[1], Mirjam B. Zeisel[4], Thierry Huby[5], Eric Rubinstein[6,7], Georges Snounou[1], Dominique Mazier[1,8], François Nosten[2,3], Thomas F. Baumert[4,9], Olivier Silvie[1]

[1]Sorbonne Universités, UPMC Univ Paris 06, INSERM, CNRS, Centre d'Immunologie et des Maladies Infectieuses, U1135, ERL8255, F-75013, Paris, France.
[2]Shoklo Malaria Research Unit, Mahidol-Oxford Tropical Medicine Research Unit, Faculty of Tropical Medicine, Mahidol University, Mae Sot, Thailand.
[3]Centre for Tropical Medicine and Global Health, Nuffield Department of Medicine Research building, University of Oxford Old Road campus, Oxford, United Kingdom.
[4]INSERM, U1110, Institut de Recherche sur les Maladies Virales et Hépatiques, F-67000, Strasbourg, France; Université de Strasbourg, F-67000, Strasbourg, France.
[5]Sorbonne Universités, UPMC Univ Paris 06, INSERM, Institute of Cardiometabolism and Nutrition, UMR_S 1166, F-75013, Paris, France.
[6]INSERM, U935, F-94807, Villejuif, France.
[7]Université Paris Sud, Institut André Lwoff, F-94807, Villejuif, France.
[8]Assistance Publique Hôpitaux de Paris, Centre Hospitalo-Universitaire Pitié- Salpêtrière, F-75013 Paris, France.
[9]Institut Hospitalo-Universitaire, Pôle Hépato-digestif, Hopitaux Universitaires de Strasbourg, F-67000 Strasbourg, France.

Correspondence and requests for materials should be addressed to OS (olivier.silvie@inserm.fr).

*CM and ST contributed equally to this study.

ABSTRACT

Plasmodium sporozoites, the mosquito-transmitted forms of the malaria parasite, first infect the liver for an initial round of replication before the emergence of pathogenic blood stages. Sporozoites represent attractive targets for antimalarial preventive strategies, yet the mechanisms of parasite entry into hepatocytes remain poorly understood. Here we show that the two main species causing malaria in humans, *Plasmodium falciparum* and *Plasmodium vivax*, rely on two distinct host cell surface proteins, CD81 and the Scavenger Receptor BI (SR-BI), respectively, to infect hepatocytes. By contrast, CD81 and SR-BI fulfil redundant functions during infection by the rodent parasite *P. berghei*. Genetic analysis of sporozoite factors reveals the 6-cysteine domain protein P36 as a major parasite determinant of host cell receptor usage. Our data provide molecular insights into the invasion pathways used by different malaria parasites to infect hepatocytes, and establish a functional link between a sporozoite putative ligand and host cell receptors.

INTRODUCTION

Hepatocytes are the main cellular component of the liver and the first replication niche for the malaria-causing parasite *Plasmodium*. Malaria begins with the inoculation of sporozoites into the host skin by infected *Anopheles* mosquitoes. Sporozoites rapidly migrate to the liver and actively invade hepatocytes by forming a specialized compartment, the parasitophorous vacuole (PV), where they differentiate into thousands of merozoites (1). Once released in the blood, merozoites invade and multiply inside erythrocytes, causing the malaria disease.

Under natural transmission conditions, infection of the liver is an essential, initial and clinically silent phase of malaria, and therefore constitutes an ideal target for prophylactic intervention strategies. However, the molecular mechanisms underlying *Plasmodium* sporozoite entry into hepatocytes remain poorly understood. Highly sulphated proteoglycans in the liver sinusoids are known to bind the circumsporozoite protein, which covers the parasite surface, and contribute to the homing and activation of sporozoites (2,3). Subsequent molecular interactions leading to sporozoite entry into hepatocytes have not been identified yet. Several parasite proteins have been implicated, such as the thrombospondin related anonymous protein (TRAP) (4), the apical membrane antigen 1 (AMA-1) (5), or the 6-cysteine domain proteins P52 and P36 (6–10), however their role during sporozoite invasion remains unclear (11).

Our previous work highlighted the central role of the host tetraspanin CD81, one of the receptors for the hepatitis C virus (HCV) (12), during *Plasmodium* liver infection (13). CD81 is an essential host entry factor for human-infecting *P. falciparum* and rodent-infecting *P. yoelii* sporozoites (13,14). CD81 acts at an early step of invasion, possibly by providing signals that trigger the secretion of rhoptries, a set of apical organelles involved in PV formation (15). Whereas CD81 binds the HCV E2 envelope protein (12), there is no evidence for such a direct interaction between CD81 and *Plasmodium* sporozoites (13). Rather, we proposed that CD81 acts indirectly, possibly by regulating an as yet unidentified receptor for sporozoites within cholesterol-dependent tetraspanin-enriched microdomains (16,17).

Intriguingly, the rodent malaria parasite *P. berghei* can infect cells lacking CD81 (13,18), however the molecular basis of this alternative entry pathway was until now totally unknown.

Another hepatocyte surface protein, the scavenger receptor BI (SR-BI), was shown to play a dual role during malaria liver infection, first in promoting parasite entry and subsequently its development inside hepatocytes (19,20). However, the contribution of SR-BI during parasite entry is still unclear. SR-BI, which is also a HCV entry factor (21,22), binds high-density lipoproteins with high affinity and mediates selective cellular uptake of cholesteryl esters (23). Yalaoui *et al*. reported that SR-BI is involved indirectly during *P. yoelii* sporozoite invasion, by regulating the levels of membrane cholesterol and the expression of CD81 and its localization in tetraspanin-enriched microdomains (19). In another study, Rodrigues *et al.* observed a reduction of *P. berghei* invasion of Huh-7 cells upon SR-BI inhibition (20). Since CD81 is not required for *P. berghei* sporozoite entry into Huh-7 cells (18), these results suggested a CD81-independent role for SR-BI. More recently, Foquet *et al*. showed that anti-CD81 but not anti-SR-BI antibodies inhibit *P. falciparum* sporozoite infection in humanized mice engrafted with human hepatocytes (24), questioning the role of SR-BI during *P. falciparum* infection.

These conflicting results prompted us to revisit the contribution of SR-BI during *P. falciparum, P. yoelii* and *P. berghei* sporozoite infections. For the first time, we also explored the role of CD81 and SR-BI during hepatocyte infection by *P. vivax*, a widely distributed yet highly neglected cause of malaria in humans, for which the contribution of hepatocyte surface receptors has not been investigated to date.

Here, we show that SR-BI is an important entry factor for *P. vivax* but not for *P. falciparum* or *P. yoelii* sporozoites. Remarkably, SR-BI and CD81 fulfil redundant functions during host cell invasion by *P. berghei* sporozoites, which can use one or the other molecule. We further investigated parasite determinants associated with host cell receptor usage. We show that genetic depletion of P52 and P36, two members of the *Plasmodium* 6-cysteine domain protein family, abrogates sporozoite productive invasion and mimics the inhibition of CD81 and/or SR-BI entry pathways, in both *P. berghei* and *P. yoelii*. Finally, we identify P36

as the molecular driver of *P. berghei* sporozoite entry via SR-BI. Our data, by revealing a functional link between parasite and host cell entry factors, pave the way towards the identification of ligand-receptor interactions mediating *Plasmodium* infection of hepatocytes, and open novel perspectives for preventive and therapeutic approaches.

RESULTS

Antibodies against SR-BI inhibit *P. vivax* but not *P. falciparum* or *P. yoelii* sporozoite infection

To evaluate the contribution of CD81 and SR-BI during *P. vivax* infection, we tested the effects of neutralizing CD81- and/or SR-BI- specific antibodies on *P. vivax* sporozoite infection in primary human hepatocyte cultures (25). A monoclonal antibody (mAb) against the main extracellular domain of CD81, previously shown to inhibit *P. falciparum* sporozoite infection (13), had no effect on the number of *P. vivax*-infected cells *in vitro* (***Figure 1A***). In sharp contrast, a mouse mAb specific for SR-BI (26) greatly reduced infection, with no additive effect of anti-CD81 antibodies (***Figure 1A***). The same inhibitory effect was observed using polyclonal anti-SR-BI antibodies (***Figure 1B***). We performed the same experiments with *P. falciparum* sporozoites and found that anti-CD81 but not anti-SR-BI antibodies inhibit *P. falciparum* infection *in vitro* (***Figure 1C***), in agreement with the *in vivo* data from Foquet *et al* (24). These data strongly suggest that *P. vivax* and *P. falciparum* sporozoites use distinct entry pathways to infect hepatocytes, reminiscent of the differences between *P. berghei* and *P. yoelii* (13).

Two distinct populations of *P. vivax* exo-erythrocytic forms (EEFs) could be distinguished in the infected cultures, large EEFs representing replicating schizonts, and small EEFs that may correspond to hypnozoites (27) (***Figure 1D***). Anti-SR-BI antibodies reduced the numbers of large and small EEFs to the same extent (***Figure 1E***), suggesting an effect on sporozoite invasion rather than on parasite intracellular development.

SR-BI is required for productive invasion of CD81-null cells by *P. berghei* sporozoites

In order to investigate in more details the role of SR-BI during sporozoite entry, we used the more tractable rodent malaria parasite *P. berghei*. Indeed, *P. berghei* sporozoites readily infect HepG2 cells, which lack CD81 (28,29) but express high levels of SR-BI (***Figure 2-figure supplement 1***), raising the possibility that this rodent parasite uses a SR-BI route to infect CD81-null cells. To test this hypothesis, *P. berghei* sporozoites constitutively

expressing GFP (PbGFP) (30) were incubated with HepG2 cells in the presence of increasing concentrations of polyclonal anti-SR-BI rabbit antibodies. We observed a dramatic and dose-dependent reduction of the number of EEF-infected cells induced by anti-SR-BI antibodies (***Figure 2A***). Quantification of host cell invasion by FACS demonstrated that the rabbit anti-SR-BI antibodies block infection at the invasion step (***Figure 2B***). Similar results were obtained with polyclonal rat antibodies and a mouse mAb directed against human SR-BI (***Figure 2-figure supplement 2***).

As a complementary approach, we used small interfering RNA (siRNA) to specifically knockdown SR-BI expression in HepG2 cells (***Figure 2D***). SR-BI silencing caused a dramatic reduction of the number of EEF-infected cells (***Figure 2E***), but had no significant effect on the intracellular development of the few invaded parasites (***Figure 2F***). *Plasmodium* sporozoites migrate through several cells before invading a final one inside a PV (31). Sporozoite cell traversal was increased in SR-BI-depleted HepG2 cells, as compared to the control (***Figure 2-figure supplement 3***). This is likely due to the robust cell traversal activity of *P. berghei* sporozoites, which continue to migrate through cells when productive invasion is impaired. Altogether, these data establish that SR-BI is a major entry factor for *P. berghei* sporozoites in CD81-null HepG2 cells.

CD81 and SR-BI play redundant roles during *P. berghei* sporozoite invasion

We next tested whether the presence of CD81 would affect SR-BI function during *P. berghei* sporozoite infection. We monitored invasion and replication of *P. berghei* sporozoites in HepG2 cells genetically engineered to express CD81 (HepG2/CD81) (***Figure 2-figure supplement 1***) (14), in the presence of anti-SR-BI and/or anti-CD81 antibodies. Strikingly, unlike in CD81-null HepG2 cells, anti-SR-BI antibodies had no inhibitory effect on *P. berghei* infection in HepG2/CD81 cells (***Figure 3A***). Remarkably, whilst neither anti-SR-BI nor anti-CD81 antibodies alone had any significant impact on invasion (***Figure 3A***) or parasite intracellular development (***Figure 3-figure supplement 1***), the combination of CD81 and SR-BI antibodies markedly reduced the number of infected cells (***Figure 3A***). Similarly,

siRNA-mediated silencing of either CD81 or SR-BI alone had no effect on infection, whereas simultaneous silencing of both factors greatly reduced infection (***Figure 3B***).

Blocking both CD81 and SR-BI was associated with an increase in cell traversal activity (***Figure 3-figure supplement 1***), suggesting that the concomitant neutralization of the two host factors prevented commitment to productive invasion. To directly test this hypothesis, we analysed the invasion kinetics of PbGFP sporozoites in HepG2/CD81 cells, in the presence of anti-SR-BI and/or anti-CD81 neutralizing antibodies. We have shown that *in vitro* sporozoite invasion follows a two-step kinetics (32), with initially low invasion rates at early time points, reflecting cell traversal activity, followed by a second phase of productive invasion associated with PV formation. In HepG2/CD81 cells, the invasion kinetics of *P. berghei* sporozoites in the presence of anti-SR-BI or anti-CD81 specific antibodies were comparable to those of the control without antibody (***Figure 3C***). In sharp contrast, blocking both CD81 and SR-BI simultaneously suppressed the second phase of productive invasion (***Figure 3C***). Based on these results, we conclude that SR-BI and CD81 are involved in the commitment to productive entry.

P. berghei sporozoites infect mouse hepatocytic Hepa1-6 cells via a CD81-dependent pathway, as shown by efficient inhibition of infection by CD81 specific antibodies or siRNA (18). Interestingly, we failed to detect SR-BI in Hepa1-6 cells (***Figure 3D***), providing a plausible explanation as to why CD81 is required for *P. berghei* infection in this model. We tested whether ectopic expression of SR-BI would rescue *P. berghei* infection of Hepa1-6 cells upon silencing of endogenous murine CD81 by siRNA. CD81-silenced Hepa1-6 cells were transiently transfected with plasmids encoding human SR-BI or CD81, before exposure to *P. berghei* sporozoites. The number of infected cells was greatly reduced in CD81-silenced cells as compared to control non-silenced cells (***Figure 3E***), in agreement with our previous observations (18). Remarkably, transfection of either human CD81 or human SR-BI was sufficient to rescue infection in CD81-silenced cells (***Figure 3E***), demonstrating that the two receptors can independently perform the same function to support *P. berghei* infection.

193 Collectively, our data provide direct evidence that CD81 and SR-BI play redundant roles
194 during productive invasion of hepatocytic cells by *P. berghei* sporozoites.
195
196 ***P. yoelii* sporozoites require host CD81 but not SR-BI for infection**
197 We next investigated the contribution of SR-BI to *P. yoelii* sporozoite infection in
198 HepG2/CD81 cells. *P. yoelii* infection was dramatically reduced by anti-CD81 antibodies,
199 consistent with our previous work (14), but strikingly was not affected by anti-SR-BI
200 antibodies (***Figure 4A***). In addition, *P. yoelii* infection was not affected by siRNA-mediated
201 silencing of SR-BI, but was almost abolished upon knockdown of CD81 (***Figure 4B***). These
202 results indicate that CD81 but not SR-BI plays a central role during *P. yoelii* sporozoite
203 invasion in HepG2/CD81 cells, similarly to *P. falciparum* in human hepatocytes.
204
205 **The 6-cysteine domain proteins P52 and P36 are required for sporozoite productive**
206 **invasion irrespective of the host cell entry pathway**
207 The data above show that *P. berghei* sporozoites can use either CD81 or SR-BI to
208 infect hepatocytic cells, whereas *P. yoelii* utilizes CD81 but not SR-BI, suggesting that one or
209 several *P. berghei* factors may be specifically associated with SR-BI usage. Among potential
210 candidate parasite factors involved in sporozoite entry, we focused on the 6-cysteine domain
211 proteins P52 and P36, two micronemal proteins of unknown function previously implicated
212 during liver infection (6–10,33,34). To facilitate monitoring of the role of P52 and P36 during
213 host cell invasion, we used a Gene Out Marker Out (GOMO) strategy (30) to generate highly
214 fluorescent *p52/p36*-knockout parasite lines in *P. berghei* (***Figure 5-figure supplement* 1**)
215 and *P. yoelii* (***Figure 5-figure supplement* 2**). Pure populations of GFP-expressing, drug
216 selectable marker-free PbΔ*p52/p36* and PyΔ*p52/p36* blood stage parasites were obtained
217 and transmitted to mosquitoes in order to produce sporozoites.
218 Analysis of the kinetics of PbΔ*p52/p36* sporozoite invasion by FACS, in comparison
219 to control PbGFP sporozoites, revealed that genetic ablation of *p52/p36* abrogates
220 sporozoite productive invasion of HepG2 (SR-BI-dependent entry pathway) and Hepa1-6

cells (CD81-dependent entry pathway) (***Figure 5A and 5B***). PbΔ*p52/p36* sporozoite invasion followed similar kinetics to those observed for PbGFP sporozoites upon blockage of SR-BI or CD81, respectively, and was not modified by addition of anti-SRBI or anti-CD81 antibodies. Using antibodies specific for UIS4, a marker of the PV membrane (PVM) that specifically labels productive vacuoles (32,35), we confirmed that PbGFP but not PbΔ*p52/p36* parasites could form replicative PVs, in both HepG2 and HepG2/CD81 cells (***Figure 5C***). In both cell types, only very low numbers of EEFs were observed with PbΔ*p52/p36* parasites (***Figure 5D***), all of which were seemingly intranuclear and lacked a UIS4-labeled PVM (***Figure 5E***). We have shown before that intranuclear EEFs result from cell traversal events (14). Altogether these data demonstrate that PbΔ*p52/p36* sporozoites fail to productively invade host cells, irrespective of the entry route. Similar results were obtained with a *P. berghei* Δ*p36* single knockout line using the GOMO strategy (***Figure 5-figure supplement* 3**). PbΔ*p36* sporozoites did not invade HepG2 cells or HepG2/CD81 cells, reproducing a similar phenotype as PbGFP parasites in the presence of anti-CD81 and anti-SR-BI neutralizing antibodies (***Figure 5-figure supplement* 4**).

We then examined the kinetics of *P. yoelii* Δ*p52/p36* sporozoite invasion, in comparison to those of PyGFP sporozoites, in HepG2/CD81 versus HepG2 cells. PyΔ*p52/p36* sporozoites showed a lack of productive invasion in HepG2/CD81 cells, reproducing the invasion kinetics of PyGFP in the CD81-null HepG2 cells (***Figure 5F***). The PyΔ*p52/p36* mutant failed to form PV in HepG2/CD81 cells (***Figure 5G***), where only intranuclear EEFs lacking a UIS4-labeled PVM were observed, similarly to the control PyGFP parasites in HepG2 cells (***Figure 5H and 5I***).

Altogether, these results reveal that P52 and/or P36 are required for sporozoite productive invasion, in both *P. berghei* and *P. yoelii,* irrespective of the entry route.

P36 is a key determinant of host cell receptor usage during sporozoite invasion

We further sought to investigate whether P52 and/or P36 proteins contribute to the selective usage of host cell receptors by different sporozoite species. We designed a trans-

249 species genetic complementation strategy in which copies of *P. berghei* (Pb), *P. yoelii* (Py),
250 *P. falciparum* (Pf) or *P. vivax* (Pv) P52 and P36 were introduced in the Δ*p52/p36* parasites.
251 For this purpose, we used centromeric plasmid constructs for stable expression of the
252 transgenes from episomes (36). Complementing PbΔ*p52/p36* sporozoites with PbP52 and
253 PbP36 restored sporozoite infectivity to both HepG2 and HepG2/CD81 cells (***Figure 6A***),
254 where the parasite formed UIS4-positive vacuoles (***Figure 6B, 6C and 6D***), confirming that
255 genetic complementation was efficient. Remarkably, complementation of PbΔ*p52/p36* with
256 PyP52 and PyP36 restored infection in HepG2/CD81 but not in HepG2 cells (***Figure 6A***),
257 where only low numbers of UIS4-negative intranuclear EEFs were observed (***Figure 6B and***
258 ***6D***). Thus, the concomitant replacement of PbP52 and PbP36 by their *P. yoelii* counterparts
259 reproduced a *P. yoelii*-like invasion phenotype in chimeric *P. berghei* sporozoites, indicating
260 that P52 and/or P36 contribute to the selective usage of a CD81-independent entry pathway
261 in *P. berghei* sporozoites. Complementation of PbΔ*p52/p36* parasites with either *P.*
262 *falciparum* or *P. vivax* P52 and P36 coding sequences did not restore infectivity of transgenic
263 sporozoites, not only in HepG2 and HepG2/CD81 cells (***Figure 6-figure supplement 1A***),
264 but also in primary human hepatocytes, the most permissive cellular system for human
265 malaria sporozoites *in vitro* (***Figure 6-figure supplement 1B***). Hence it was not possible
266 using this approach to assess the function of *P. falciparum* or *P. vivax* P52 and P36 in
267 transgenic *P. berghei* sporozoites.

268 We next dissected the individual contribution of P52 and P36 by complementing
269 PbΔ*p52/p36* parasites with mixed combinations of either PyP52 and PbP36 or PbP52 and
270 PyP36. This approach revealed that P36 determines the ability of *P. berghei* sporozoites to
271 enter cells via a CD81-independent route. Indeed, PbΔ*p52/p36* complemented with PyP52
272 and PbP36 infected both HepG2/CD81 and HepG2 cells (***Figure 6A***), forming UIS4-labeled
273 PVs in both cell types (***Figure 6B, 6C and 6D***). P52 therefore is not responsible for the
274 phenotypic difference between *P. berghei* and *P. yoelii*. In sharp contrast, complementation
275 of PbΔ*p52/p36* with PbP52 and PyP36 restored sporozoite infectivity to HepG2/CD81 but not
276 HepG2 cells, thus reproducing a *P. yoelii*-like invasion phenotype (***Figure 6A, 6B and 6D***).

In reciprocal experiments, we analysed whether expression of PbP36 would be sufficient to allow *P. yoelii* sporozoites to invade CD81-null cells. For this purpose, we performed genetic complementation experiments in Py*Δp52/p36* parasites, using the same constructs employed with the *P. berghei* mutant. Strikingly, whilst HepG2 cells are normally refractory to *P. yoelii* productive invasion, complementation with *P. berghei* P52 and P36 protein was sufficient to confer chimeric *P. yoelii* mutants the capacity to infect HepG2 cells (***Figure 7A***). Most importantly, Py*Δp52/p36* parasites complemented with PyP52 and PbP36 infected both HepG2 and HepG2/CD81 cells (***Figure 7A***). In particular, Py*Δp52/p36* parasites expressing PbP36 became capable of forming UIS4-positive PVs in HepG2 cells (***Figure 7B***). Thus, the transgenic expression of PbP36 appears to be sufficient to recapitulate a *P. berghei*-like invasion phenotype in *P. yoelii* sporozoites. In contrast, complementation of Py*Δp52/p36* parasites with PbP52 and PyP36 restored sporozoite infectivity in HepG2/CD81 cells only, but not in HepG2 cells (***Figure 7A and 7B***). This confirms that P52, although essential for sporozoite entry, is not directly associated with host receptor usage. Finally, invasion of PbP36-expressing Py*Δp52/p36* sporozoites was abrogated by anti-SR-BI antibodies in HepG2 cells (***Figure 7C***), demonstrating that *P. berghei* P36 is a key determinant of CD81-independent entry via SR-BI.

DISCUSSION

Until now, the nature of the molecular interactions mediating *Plasmodium* sporozoite invasion of hepatocytes has remained elusive. Previous studies have identified CD81 and SR-BI as important host factors for infection of hepatocytes (13,19,20). Still, the relation between CD81 and SR-BI and their contribution to parasite entry was unclear (18,24), and, importantly, parasite factors associated with CD81 or SR-BI usage had not been identified. Here we demonstrate that CD81 and SR-BI define independent entry pathways for sporozoites, and identify the parasite protein P36 as a critical parasite factor that determines host receptor usage during hepatocyte infection.

Our data provide molecular insights into the host entry pathways used by different sporozoite species (***Figure 8A***). We show that *P. falciparum*, like *P. yoelii*, relies on CD81 but not SR-BI, in agreement with the recent observation that antibodies against CD81 but not anti-SR-BI induce protection in humanized mice infected with *P. falciparum* (24). Our results are also consistent with the study from Yalaoui *et al.* showing that in primary mouse hepatocytes antibodies against SR-BI do not inhibit *P. yoelii* infection when co-incubated together with sporozoites (19). In the same study, the authors proposed a model where SR-BI indirectly contributes to *P. yoelii* infection through regulation of membrane cholesterol and CD81 expression, however our data in the HepG2/CD81 cell model with both *P. yoelii* and *P. berghei* clearly rule out a role of SR-BI during CD81-dependent sporozoite entry. For the first time, we also analysed the role of host factors during *P. vivax* sporozoite infection. We found that, in contrary to *P. falciparum*, antibodies against SR-BI but not against CD81 inhibit infection of primary human hepatocyte cultures by *P. vivax* sporozoites, illustrating that the two main species causing malaria in humans use distinct routes to infect hepatocytes.

SR-BI and CD81 both have been shown to bind the HCV envelope glycoprotein E2 (12,21,22), and act in a sequential and cooperative manner to mediate virus entry (37), together with several additional entry factors (38–40). By contrast, as shown here, SR-BI and CD81 operate independently during *Plasmodium* sporozoite infection. Remarkably, *P. berghei* can use alternatively CD81 or SR-BI to infect cells, which is surprising given that

CD81 and SR-BI are structurally unrelated. CD81 belongs to the family of tetraspanins, which are notably characterized by their propensity to dynamically interact with other membrane proteins and organize tetraspanin-enriched membrane microdomains (41). CD81 might play an indirect role during *Plasmodium* sporozoite entry, possibly by interacting with other host receptors within these microdomains (16,17,42). Interestingly, SR-BI is structurally related to CD36 (43), which is known to bind several *Plasmodium* proteins, including *P. falciparum* erythrocyte membrane protein 1 (PfEMP1) in the context of cytoadherence of infected erythrocytes to endothelial cells (44–46). CD36 was also reported to interact with *P. falciparum* sequestrin (also called LISP2) (47), a member of the 6-cys protein family involved in parasite liver stage development (48,49), and is a major determinant of *P. berghei* asexual blood stage sequestration (50). CD36 was shown to be dispensable for mouse hepatocyte infection by *P. yoelii* and *P. berghei* sporozoites (51). However, it is conceivable that SR-BI, which shares a similar 3D structure as CD36 (43), may interact with parasite proteins expressed by sporozoites, such as the 6-cys protein P36.

The 6-cys protein family is characterized by the presence of a cysteine-rich domain, the 6-cysteine (6-cys) or s48/45 domain. *Plasmodium* spp. possess a dozen 6-cys proteins, which perform important functions in different life cycle stages, and are often located on the parasite surface, consistent with a role in cellular interactions (49). Previous studies have shown that *Plasmodium* P52 and P36 are crucial for infection of the liver by sporozoites (6–8), although it remained unclear whether their role was at the sporozoite entry step (7,10) or for maintenance of the PV post-entry (6,33,34). It should be noted that standard invasion assays, as performed in these studies, do not distinguish between sporozoite productive entry and non-productive invasion events associated with cell traversal, complicating the interpretation of phenotypic analysis of the mutants. Here, using GFP-expressing *p52* and *p36* mutants and a robust FACS-based invasion assay (32), we unequivocally establish that *P. yoelii* and *P. berghei* sporozoites lacking P52 and P36 efficiently migrate through cells but do not commit to productive invasion, reproducing the phenotype observed upon blockage of CD81 or SR-BI.

Using a trans-species genetic complementation strategy, we identified P36 as a crucial parasite determinant of host receptor usage. Our data, combined with previous studies (6–9), demonstrate that both P36 and P52 are necessary for sporozoite infection of hepatocytes, irrespective of the invasion route used by the parasite. Our study now reveals that P36 but not P52 is responsible for the phenotypic differences between *P. berghei* and *P. yoelii* sporozoites regarding host cell entry pathways. Importantly, *P. berghei* P36 mediates sporozoite entry via either CD81 or SR-BI, whereas *P. yoelii* P36 only supports CD81-dependent invasion (***Figure 8B***). These results strongly suggest that PbP36 contains specific structural determinants that confer the ability of the protein to interact with SR-BI or SR-BI-dependent molecules. *P. berghei* and *P. yoelii* P36 proteins share 88% identity and 97% similarity in their amino acid sequence (***Figure 8-figure supplement* 1**). Structural modelling of PbP36, using the crystal structure of the 6-cys protein PfP12 (52) as a template, shows a typical beta sandwich fold for each of the tandem 6-cysteine domains (***Figure 8C***). Most of the divergent residues between PbP36 and PyP36 are located in the second 6-cys domain (***Figure 8-figure supplement* 1**), including in a loop located between the third and fourth cysteine residues. In this particular loop, PfP36 and PvP36 contain an inserted sequence of 21 and 3 amino acids, respectively, which may affect their binding properties and functions.

Single gene deletions of *p52* or *p36* result in similar phenotypes as *p52/p36* double knockouts, suggesting that the two proteins act in concert (6–8,10). In *P. falciparum* blood stages, the two 6-cys proteins P41 and P12 interact to form stable heterodimers on the surface of merozoites (52–54). Whilst P12 is predicted to be GPI-anchored, P41 lacks a membrane-binding domain, similarly to P36. By analogy, we hypothesize that P36 may form heterodimers with other GPI-anchored 6-cys proteins, including P52. Our data show that complementation of Pb*Δp52/p36* parasites with P52 and P36 from *P. falciparum* or *P. vivax* does not restore sporozoite infectivity, supporting the idea that other yet unidentified parasite factors cooperate with P52 and P36 during invasion. In addition to P52 and P36, sporozoites express at least three other 6-cys proteins, B9, P12p and P38 (55,56). Whereas gene deletion of *p38* causes no detectable phenotypic defect in *P. berghei* (57), B9 has been

379 shown to play a critical role during liver stage infection, not only in *P. berghei* but also in *P.*
380 *yoelii* and *P. falciparum* (49). Whether B9, P38 and P12p associate with P52 and/or P36 and
381 contribute to sporozoite invasion still deserves further investigations.

382 Several 6-cys proteins have been implicated in molecular interactions with host
383 factors. As mentioned above, sequestrin was reported to interact with CD36 (47), although
384 the functional relevance of this interaction remains to be determined, as sequestrin is only
385 expressed towards the end of liver stage development (48). Recent studies have shown that
386 *P. falciparum* merozoites evade destruction by the human complement through binding of
387 host factor H to the 6-cys protein Pf92 (58,59). Pfs47 expressed by *P. falciparum* ookinetes
388 plays a critical role in immune evasion in the mosquito midgut, by suppressing nitration
389 responses that activate the complement-like system (60,61). Pfs47 was proposed to act as a
390 “key” that allows the parasite to switch off the mosquito immune system by interacting with
391 yet unidentified mosquito receptors (“lock”) (62). By analogy, based on our results, one could
392 envisage P36 as a crucial determinant of a sporozoite “key” that opens SR-BI and/or CD81-
393 dependent “locks” for entry into hepatocytes.

394 The function of P36 interaction with host cell receptors remains to be defined. P36
395 binding to SR-BI and/or CD81, either directly or indirectly, may participate in a signalling
396 cascade that triggers rhoptry secretion and assembly of the moving junction, key events
397 committing the parasite to host cell entry (63). Alternatively, P36 may induce signalling in the
398 host cell by acting on SR-BI or other hepatocyte receptors. In this regard, Kaushansky *et al*.
399 recently reported that sporozoites preferentially invade host cells expressing higher levels of
400 the EphA2 receptor (9). Interestingly, this preference was still observed with *p52*/*p36*-
401 deficient parasites, strongly suggesting that there is no direct link between EphA2 and
402 P52/P36-dependent productive invasion. However, the same study showed that P36
403 interferes with Ephrin A1-mediated EphA2 phosphorylation (9), raising the possibility that
404 P36 may affect EphA2 signalling indirectly, for example via SR-BI and the SRC pathway
405 (64,65).

406 In conclusion, our study reveals that host CD81 and SR-BI define two alternative
407 pathways in human cells for sporozoite entry. Most importantly, we identified the parasite 6-
408 cysteine domain protein P36 as a key determinant of host receptor usage during infection.
409 These results pave the way toward the elucidation of the mechanisms of sporozoite invasion.
410 The identification of the parasite ligands that mediate host cell entry may provide potential
411 targets for the development of next-generation malaria vaccines. P36 is required for both
412 CD81- and SR-BI-dependent sporozoite entry, suggesting that it may represent a relevant
413 target in both *P. falciparum* and *P. vivax*. The understanding of host-parasite interactions
414 may also contribute to novel therapeutic approaches. SR-BI-targeting agents have entered
415 clinical development for prevention of HCV graft infection (66). Our data suggest that SR-BI-
416 targeting strategies may be effective to prevent establishment of the liver stages of *P. vivax*,
417 including the dormant hypnozoite forms.
418

METHODS

Experimental animals, parasites and cells

We used wild type *P. berghei* (ANKA strain, clone 15cy1) and *P. yoelii* (17XNL strain, clone 1.1), and GFP-expressing PyGFP and PbGFP parasite lines, obtained after integration of a GFP expression cassette at the dispensable *p230p* locus (30). *P. berghei* and *P. yoelii* blood stage parasites were propagated in female Swiss mice (6–8 weeks old, from Janvier Labs). *Anopheles stephensi* mosquitoes were fed on *P. berghei* or *P. yoelii*-infected mice using standard methods (Ramakrishnan et al., 2013), and kept at 24°C and 21°C, respectively. *P. berghei* and *P. yoelii* sporozoites were collected from the salivary glands of infected mosquitoes 21–28 or 14–18 days post-feeding, respectively. *A. stephensi* mosquitoes infected with *P. falciparum* sporozoites (NF54 strain) were obtained from the Department of Medical Microbiology, University Medical Centre, St Radboud, Nijmegen, the Netherlands. *P. vivax* sporozoites were isolated from *A. cracens* mosquitoes, 15-21 days after feeding on blood from infected patients on the Thailand-Myanmar border, as described (67). HepG2 (ATCC HB-8065), HepG2/CD81 (14) and Hepa1-6 cells (ATCC CRL-1830) were checked for the absence of mycoplasma contamination and cultured at 37°C under 5% CO_2 in DMEM supplemented with 10% fetal calf serum and antibiotics (Life Technologies), as described (18). HepG2 and HepG2/CD81 were cultured in culture dishes coated with rat tail collagen I (Becton-Dickinson, Le Pont de Claix, France). Primary human hepatocytes were isolated and cultured as described previously (5).

In vitro infection assays

Primary human hepatocytes (5 x 10^4 per well in collagen-coated 96-well plates) were infected with *P. vivax* or *P. falciparum* sporozoites (3 x 10^4 per well), as described (5), and cultured for 5 days before fixation with cold methanol and immunolabeling of EEFs with antibodies specific for *Plasmodium* HSP70 (68). Nuclei were stained with Hoechst 33342 (Life Technologies). Host cell invasion by GFP-expressing *P. berghei* and *P. yoelii* sporozoites was monitored by flow cytometry (69). Briefly, hepatoma cells (3 x 10^4 per well in

collagen-coated 96-well plates) were incubated with sporozoites (5 x 10^3 to 1 x 10^4 per well). At different time points, cell cultures were washed, trypsinized and analyzed on a Guava EasyCyte 6/2L bench cytometer equipped with a 488 nm laser (Millipore), for detection of GFP-positive cells. To assess liver stage development, HepG2 or HepG2/CD81 cells were infected with GFP-expressing sporozoites and cultured for 24-36 hours before analysis either by FACS or by fluorescence microscopy, after fixation with 4% PFA and staining with antibodies specific for UIS4 (Sicgen) and Hoechst 33342. For antibody-mediated inhibition assays, we used polyclonal antisera against human SR-BI raised after genetic immunization of rabbits and rats (70,71), and monoclonal antibodies against human SR-BI (NK-8H5-E3) (26), human CD81 (1D6, Abcam) or mouse CD81 (MT81)(16).

Small interfering RNA and plasmid transfection

We used small double stranded RNA oligonucleotides targeting human CD81 (5'-GCACCAAGTGCATCAAGTA-3'), human SR-BI (5'-GGACAAGTTCGGATTATTT-3') or mouse CD81 (5'-CGTGTCACCTTCAACTGTA-3'). An irrelevant siRNA oligonucleotide targeting human CD53 (5'-CAACTTCGGAGTGCTCTTC-3') was used as a control. Transfection of siRNA oligonucleotides was performed by electroporation, as described (14). Following siRNA transfection, cells were cultured for 48 hours before flow cytometry analysis or sporozoite infection. Transfection of pcDNA3 plasmids encoding human CD81 (72) or SR-BI (70) was performed 24 hours after siRNA using the Lipofectamine 2000 reagent (Invitrogen) according to the manufacturer's specifications. Following plasmid transfection, cells were cultured for an additional 24 hours before sporozoite infection.

Constructs for targeted gene deletion of *p52* and *p36*

PbΔ*p52p36* and PbΔ*p36* mutant parasites were generated using a ''Gene Out Marker Out'' strategy (30). For generation of PbΔp52p36 parasites, a 5' fragment of PbP52 gene (PBANKA_1002200) and a 3' fragment of PbP36 gene (PBANKA_1002100) were amplified by PCR from P. berghei ANKA WT genomic DNA, using primers PbP52rep1for (5'-

TCCCCGCGGAATCGTGATGCTATGGATAACGTAACAC-3'), PbP52rep2rev (5'-ATAAGAATGCGGCCGCAAAAAGAGACAAACACACTTTGTGAACACC-3'), PbP36rep3for (5'-CCGCTCGAGTTAATATGTGATGTGTGTAGAAGAGTGAGG-3') and PbP36rep4rev (5'-GGGGTACCTTGATATACATGCAACTTTTCACATAGG-3'), and inserted into SacII/NotI and XhoI/KpnI restriction sites, respectively, of the GOMO-GFP vector1. For generation of PbΔp36 parasites, a 5' and a 3' fragment of PbP36 gene were amplified by PCR from P. berghei ANKA WT genomic DNA, using primers PbP36repAfor (5'-AGCTGGAGCTCCACCGCGGGAAAAAAGGTTAACACATATATTGAAAAGC-3'), PbP52rep-Arev (5'-CGGCTGAGGGCGGCCGCAATCAAAAAAAATAATAAAAACAAATATATGTACAC-TCG-3'), and PbP36repBfor (5'-ATTAATTTCACTCGAGTATGTGATGTGTGTAGAAGAGT-GAGG-3') and PbP36repBrev (5'-TATAGGGCGAATTGGGTACCGCACGCCGGAAAAATTA-CAATACAAATGG-3'), and inserted into SacII/NotI and XhoI/KpnI restriction sites, respectively, of the GOMO-GFP vector using the In-Fusion HD Cloning Kit (Clontech).

For generation of PyΔp52p36 parasites, 5' and 3' fragments of PyP52 gene (PY17X_1003600) and a 3' fragment of PyP36 gene (PY17X_1003500) were amplified by PCR from P. yoelii 17XNL WT genomic DNA, using primers PyP52rep1for (5'-TCCCCG-CGGAATCGCCATGCTATGGATAGTGTAGC-3'), PyP52rep2rev (5'-ATAAGAATGCGGCC-GCCATTGAAGGGGGGAACAAATCGACG-3'), PyP52rep3for (5'-CCGCTCGAGTCAATAT-ATGCCCACTATTCGAATTTTTGG-3'), PyP52rep4rev (5'-GGGGTACCTTATTGATATGC-ATGCAACTTTCACATAGG-3'), PyP36repFor (5'-ATAAGAATGCGGCCGCAAAATGCAA-GGCGCCCGTTTAGAACC-3') and PyP36repRev (5'-CCGGAATTCACAAAAAGATGC-TACTGTGAAAAGCTCACC-3'). The fragments were inserted into SacII/NotI, XhoI/KpnI and NotI/EcoRI restriction sites, respectively, of a GOMO vector backbone containing mCherry and hDHFR-yFCU cassettes. The resulting targeting constructs were verified by DNA sequencing (GATC Biotech), and were linearized with SacII and KpnI before transfection.

Wild type *P. berghei* ANKA blood stage parasites were transfected with *pbp52p36* and *pbp36* targeting constructs using standard transfection methods (Janse et al., 2006). GFP-expressing parasite mutants were isolated by flow cytometry after positive and negative

503 selection rounds, as described(30). PyGFP blood stage parasites were transfected with a
504 *pyp52pyp36* targeting construct and a GFP-expressing drug selectable marker-free
505 PyΔ*p52p36* mutant line was obtained using a two steps “Gene Out Marker Out” strategy.
506 Correct construct integration was confirmed by analytical PCR using specific primer
507 combinations.
508
509 **Constructs for genetic complementation of Δ*p52p36* mutants**
510 For genetic complementation experiments, we used centromeric plasmids to achieve stable
511 transgene expression from episomes (36). Complementation plasmids were obtained by
512 replacing the GFP cassette of pCEN-SPECT2 plasmid (kindly provided by Dr S. Iwanaga)
513 with a P52/P36 double expression cassette. Four complementing plasmids were generated,
514 allowing expression of PbP52/PbP36, PyP52/PyP36, PbP52/PyP36 or PyP52/PbP36.
515 The centromeric plasmid constructs were assembled by In-Fusion cloning of 4 fragments in
516 two-steps, into KpnI/SalI restriction sites of the pCEN-SPECT2 plasmid. For this purpose,
517 fragments corresponding to the promoter region of PbP52 (insert A, 1.5 kb), the open
518 reading frame (ORF) of PbP52 (insert B, 1.7 kb), the 3’ untranslated region (UTR) of PbP52
519 and promoter region of PbP36 (insert C, 1.5 kb), the ORF and 3’ UTR of PbP36 (insert D, 2
520 kb), the promoter region of PyP52 (insert E, 1.5 kb), the open reading frame (ORF) of PyP52
521 (insert F, 1.7 kb), the 3’ untranslated region (UTR) of PyP52 and promoter region of PyP36
522 (insert G, 1.6 kb), and the ORF and 3’ UTR of PyP36 (insert H, 2 kb) were first amplified by
523 PCR from P. berghei or P. yoelii WT genomic DNA, using the following primers: Afor (5’-
524 TATAGGGCGAATTGGGTACCTTCACATGCATAAACCCGAAGTGTGC-3’), Arev (5’-
525 GAAAAAAGCAGCTAGCTTGCTTTAATGTAGAAAAAATATTTATGGATTTGG-3’), Bfor (5’-
526 ATTAAAGCAAGCTAGCAATATTACATTTGTGGTAAGGTAAAAC-3’), Brev (5’-GAAGAG-
527 GTACCAAAAAGGTTTTGCCAAAATG-3’), Cfor (5’-TTTTGGTACCTCTTCTTCTTATTATGA-
528 GG-3’), Crev (5’-GAAAAAAGCAGCTAGCAGAAAGAAACAACAGTTATCGTAATAAAG-3’),
529 Dfor (5’-GCTAGCTGCTTTTTTCTTGAATCGACAATTATAATACTGAGGC-3’), Drev (5’-
530 TACAAGCATCGTCGACATTGCCATTACAATATGCTATAATCTG-3’), Efor (5’-TATAGG-

GCGAATTGGGTACCTGCACATGCATAAACTCGAAGTGTGC-3'), Erev (5'-AAAAAAGCAG-CTAGCTTGCTTTAATGTAGAAAAAATATTTATGTATTTGG-3'), Ffor (5'-ATTAAAGCAAGC-TAGAATATTGCATTTGTGGTAAGGCAAATC-3'), Frev (5'-GAAGACGTACCAAACATA-TTTTGCCAAAATG-3'), Gfor (5'-GTTTGGTACGTCTTCTTCTTATTATGAGG-3'), Grev (5'-GAAAAAAGCAGCTAGGATAACTGTCGATTCAAAGAAACAACC-3'), Hfor (5'-GCTAG-CTGCTTTTTTATACTTGAAGCATTTTTGTTGACTCTACC-3'), Hrev (5'-TACAAGCATCGT-CGACATTACCATTACGATATGCTATAATCTG-3'). Cloning of fragments A and D followed by B and C into the pCEN vector resulted in the PbP52/PbP36 complementation plasmid. Cloning of fragments E and H followed by F and G into the pCEN vector resulted in the PyP52/PyP36 complementation plasmid. Cloning of fragments A and D followed by F and G into the pCEN vector resulted in the PyP52/PbP36 complementation plasmid. Cloning of fragments E and H followed by B and C into the pCEN vector resulted in the PbP52/PyP36 complementation plasmid. The centromeric plasmids for expression of *P. falciparum* and *P. vivax* P52 and P36 were assembled by In-Fusion cloning of 5 fragments in two steps. For this purpose, fragments corresponding to the promoter region of *PbP52* (insert B1, 1.9 kb), the 3' UTR of *PbP52* and promoter region of *PbP36* (insert B2, 1.6 kb), the 3' UTR of *PbP36* (insert B3, 2 kb), the ORF of *PfP52* (insert F1, 1.4 kb), the ORF of *PfP36* (insert F2, 1.1 kb), the ORF of *PvP52* (insert V1, 1.4 kb) and the ORF of *PvP36* (insert V2, 1.1 kb), were first amplified by PCR from *P. berghei*, *P. falciparum* or *P. vivax* genomic DNA, using the following primers: B1for (5'-TATAGGGCGAATTGGGTACCTTCACATGCATAAACCCGAA-GTGTGC-3'), B1rev (5'-GCTAGCTTACTATTATTCTCAAAATGTGTATCACATTG-3'), B2for (5'-ATCACAATA-TGTGCATAGTGTCAATATGCC-3'), B2rev (5'-AATCAAAAAAAATAATAAAAACAAATATAT-GTACACTCG-3'), B3for (5'-TAATAGTAAGCTAGCTATGTGATGTGTGTAGAAGAGTG-AGGGAG-3'), B3rev (5'-TACAAGCATCGTCGACATTGCCATTACAAT-ATGCTATAATCTG-3'), F1for (5'-ATAATAGTAAGCTAGCAAAATGTATGTATTG-GTGCTTATTCATATGTG-3'), F1rev (5'-TGCACATATTGTGATTTATGTTGAATATATATATATTAAAAATATGAATAATA-TTAAG-3'), F2for (5'-TTATTTTTTTTGATTATGGCTTATAATATTTGGGAGGAATATATAA-TGG-3'),

559 F2rev (5'-ACATCACATAGCTAGCCTAACTTTCTACAGTTTTATTTATGTTA-AATAAACC-3'),
560 V1for (5'-ATAATAGTAAGCTAGCAAAATGAGGCGGATTCTGCTGGGCTG-CTTGG-3'),
561 V1rev (5'-TGCACATATTGTGATTTACAGGG-ACGAGAAACCCGCGTAG-3'), V2for (5'-
562 TTATTTTTTTTGATTATGAGCACATGCCTTC-CAGTAGTGTGG-3'), and V2rev (5'-
563 ACATCACATAGCTAGCTCACACCGCTTCAACC-GCTGCG-3'). An intermediate vector was
564 first assembled by cloning inserts B1 and B3 into *Kpn*I/*Sal*I restriction sites of the pCEN-
565 SPECT2 plasmid. Subsequently, In-Fusion cloning of inserts F1, B2 and F2 or inserts V1, B2
566 and V2 into the *Nhe*I restriction site of the intermediate vector resulted into PfP52/PfP36 and
567 PvP52/PvP36 expression centromeric plasmids, respectively. All constructs were verified by
568 DNA sequencing (GATC Biotech) before transfection.
569
570 **Parasite transfection and selection**
571 For double crossover replacement of P52 and P36 genes and generation of the Pb*Δp52p36*,
572 Pb*Δp36* and Py*Δp52p36* parasite lines, purified schizonts of wild type *P. berghei* ANKA or
573 PyGFP were transfected with 5-10 µg of linearized construct by electroporation using the
574 AMAXA NucleofectorTM device (program U33), as described elsewhere (73), and
575 immediately injected intravenously in the tail of one mouse. The day after transfection,
576 pyrimethamine (70 or 7 mg/L for *P. berghei* and *P. yoelii*, respectively) was administrated in
577 the mouse drinking water, for selection of transgenic parasites. Pure transgenic parasite
578 populations were isolated by flow cytometry-assisted sorting of GFP and mCherry-
579 expressing blood stage parasites FACSAria II (Becton-Dickinson), transferred into naïve
580 mice, treated with 1 mg/ml 5-fluorocytosine (Meda Pharma) in the drinking water, and sorted
581 again for selection of GFP+ parasites only, as described (30). In the case of the Py*Δp52p36*
582 mutant, GFP^+ $mCherry^+$ recombinant parasites were first cloned by injection of limiting
583 dilutions into mice prior to the negative selection step. For genetic complementation of the
584 mutants, purified schizonts of Pb*Δp52p36* and Py*Δp52p36* parasites were transfected with 5
585 µg of centromeric plasmids, followed by positive selection of transgenic parasites with
586 pyrimethamine, as described above.

587

588 **Parasite genotyping**

589 Parasite genomic DNA was extracted using the Purelink Genomic DNA Kit (Invitrogen), and
590 analysed by PCR using primer combinations specific for WT and recombined loci. For
591 genotyping of Pb*Δp52p36* parasites, we used primer combinations specific for the WT Pb*p52*
592 locus (5'-AATGAGATGTCAAAAAATATAGTGCTTCC-3' and 5'-
593 AAATGAGCAGTTTCTTCTACG-TTGTTTCC-3'), for the 5' region of the recombined locus
594 (5'-TATGTTTGGAATATCAGG-ACAAGGCATGG-3' and 5'-
595 TAATAATTGAGTCTTTAGTAACGAATTGCC-3'), and for the 3' region of the recombined
596 locus before (5'-ATCGTGGAACAGTACGAACGCGCCGAGG-3' and 5'-
597 ATTGGACGTTTATTATTATTGCAAAAGCG-3') or after excision of the selectable marker (5'-
598 GATGGAAGCGTTCAACTAGCAGACC-3' and 5'-ATTGGACGTTTATTATT-
599 ATTGCAAAAGCG-3'). For genotyping of Pb*Δp36* parasites, we used primer combinations
600 specific for the WT Pb*p36* locus (5'-GAGTTCGCACGCCATATTAACACG-3' and 5'-
601 CCATGATGAGATGCTAAATCGGG-3'), for the 5' region of the recombined locus (5'-
602 GGAAGCATCATACAAAAAAGAAAGC-3' and 5'-TAATAATTGAGTCTTTAGTAAC-
603 GAATTGCC-3'), and for the 3' region of the recombined locus before (5'-
604 ATCGTGGAACAGTACGAACGCGCCGAGG-3' and 5'-CGTTATCTCTTTTTTTACTCATTAA-
605 GTATTG-3') or after excision of the selectable marker (5'-
606 GATGGAAGCGTTCAACTAGCAGACC-3' and 5'-CGTTATCTCTTTTTTTACTCATTA-
607 AGTATTG-3'). For genotyping of Py*Δp52p36* parasites, we used primer combinations
608 specific for the WT PyP52 locus (5'-ACTATATTTCAATTGGAGACATGTGG-3' and 5'-
609 ATGCAAAAAAAAGTTATCATTGCTAGTTGG-3'), for the 5' region of the recombined locus
610 (5'-GTATGTTTGGAATGCCAGGATATGACATGG-3' and 5'-CCGGAATTCACAAAAA-
611 GATGCTACTGTGAAAAGCTCACC-3'), and for the 3' region of the recombined locus before
612 (5'-AGTTACACGTATATTACGCATACAACGATG-3' and 5'-TAAGCATATATTGTATATTTG-
613 CCTTGTCC-3') or after excision of the selectable marker (5'-

GTATGTTTGGAATGCCAGGATATGACATGG-3' and 5'-AATCTGATATGATAAATTATG-GTATTGGAC-3').

Bioinformatic and structural analysis

Amino-acid sequences of the P36 proteins from *P. falciparum* (379 aa, gi:296004390, PF3D7_0404400), *P. vivax* (320 aa, gi:156094683, PVX_001025), *P. berghei* (352 aa, gi:991456178, PBANKA_1002100) and *P. yoelii* (356 aa, gi:675237743, PY17X_1003500) were obtained from Genbank. Sequence alignments were carried out using Clustal Omega (http://www.ebi.ac.uk/Tools/msa/clustalo/). A 3D model of *P. berghei* P36 was generated by the prediction program I-Tasser (74), using the 3D structure of Pf12 (Pf12short in ref (52)), which contains two 6-cys domains D1 and D2 arranged in tandem, as a template (PDB access code 2YMO). The 3D model for PbP36 was then superimposed to the template Pf12short and visually inspected using the program Coot (75), and the rotamers for the Cys residues adjusted such that the three disulfides bonds for each domain were formed following the pattern C1-C2, C3-C6 and C4-C5.

Statistical analysis

Statistical significance was assessed by non-parametric analysis using the Mann-Whitney U and Kruskal-Wallis tests. All statistical tests were computed with GraphPad Prism 5 (GraphPad Software). Significance was defined as $p<0.05$ (ns, statistically non-significant; *$p<0.05$; **$p<0.01$). *In vitro* experiments were performed at least three times, with a minimum of three technical replicates per experiment.

Ethics statement

All animal work was conducted in strict accordance with the Directive 2010/63/EU of the European Parliament and Council 'On the protection of animals used for scientific purposes'. The protocol was approved by the Charles Darwin Ethics Committee of the University Pierre et Marie Curie, Paris, France (permit number Ce5/2012/001). Blood samples were obtained

from *P. vivax*-infected individuals attending the Shoklo Malaria Research Unit (SMRU) clinics on the western Thailand-Myanmar border, after signature of a consent form(67). Primary human hepatocytes were isolated from healthy parts of human liver fragments, which were collected from adult patients undergoing partial hepatectomy (Service de Chirurgie Digestive, Hépato-Bilio-Pancréatique et Transplantation Hépatique, Groupe Hospitalier Pitié-Salpêtrière, Paris, France). The collection and use of this material were undertaken in accordance with French national ethical guidelines under Article L. 1121-1 of the 'Code de la Santé Publique', and approved by the Institutional Review Board (Comité de Protection des Personnes) of the Centre Hospitalo-Universitaire Pitié-Salpêtrière, Assistance Publique-Hôpitaux de Paris, France.

ACKNOWLEDGEMENTS

We thank Maurel Tefit, Thierry Houpert, Prapan Kittiphanakun and Saw Nay Hsel for rearing of mosquitoes in Paris and at SMRU; Geert-Jan van Gemert and Robert W. Sauerwein for providing *P. falciparum*-infected mosquitoes; Bénédicte Hoareau-Coudert (Flow Cytometry Core CyPS) for parasite sorting by flow cytometry; Valérie Soulard, Audrey Lorthiois and Morgane Mitermite for technical assistance; Maryse Lebrun for critically reading the manuscript; and Shiroh Iwanaga for kindly providing the pCEN-SPECT2 plasmid. This work was funded by the European Union (FP7 Marie Curie grant PCIG10-GA-2011-304081, FP7 PathCo Collaborative Project HEALTH-F3-2012-305578, ERC-AdG-2014-671231-HEPCIR, FP7 HepaMab, and Interreg IV-Rhin Supérieur-FEDER Hepato-Regio-Net 2012, H2020-2015-667273-HEP-CAR), the Laboratoires d'Excellence ParaFrap and HepSYS (ANR-11-LABX-0024 and ANR-10-LABX-0028), and the National Centre for the Replacement, Refinement & Reduction of Animals in Research (NC3Rs, project grant NC/L000601/1). SMRU is part of the Mahidol-Oxford University Research Unit supported by the Wellcome Trust of Great Britain. GM and MG were supported by a "DIM Malinf" doctoral fellowship awarded by the Conseil Régional d'Ile-de-France.

COMPETING FINANCIAL INTERESTS STATEMENT

The authors declare no competing financial interests.

CORRESPONDING AUTHOR

Correspondence and requests for materials should be addressed to OS (olivier.silvie@inserm.fr).

679 **REFERENCES**

680 1. Ménard R, Tavares J, Cockburn I, Markus M, Zavala F, Amino R. Looking
681 under the skin: the first steps in malarial infection and immunity. Nat Rev
682 Microbiol. 2013;11(10):701–12.
683 2. Frevert U, Sinnis P, Cerami C, Shreffler W, Takacs B, Nussenzweig V. Malaria
684 circumsporozoite protein binds to heparan sulfate proteoglycans associated
685 with the surface membrane of hepatocytes. J Exp Med. 1993;177(5):1287–98.
686 3. Coppi A, Tewari R, Bishop JR, Bennett BL, Lawrence R, Esko JD, et al.
687 Heparan Sulfate Proteoglycans Provide a Signal to Plasmodium Sporozoites to
688 Stop Migrating and Productively Invade Host Cells. Cell Host Microbe.
689 2007;2(5):316–27.
690 4. Matuschewski K, Nunes AC, Nussenzweig V, Menard R. Plasmodium
691 sporozoite invasion into insect and mammalian cells is directed by the same
692 dual binding system. Embo J. 2002;21(7):1597–606.
693 5. Silvie O, Franetich JF, Charrin S, Mueller MS, Siau A, Bodescot M, et al. A role
694 for apical membrane antigen 1 during invasion of hepatocytes by Plasmodium
695 falciparum sporozoites. J Biol Chem. 2004;279(10):9490–6.
696 6. van Dijk MR, Douradinha B, Franke-Fayard B, Heussler V, van Dooren MW,
697 van Schaijk B, et al. Genetically attenuated, P36p-deficient malarial
698 sporozoites induce protective immunity and apoptosis of infected liver cells.
699 Proc Natl Acad Sci U S A. 2005 Aug 23;102(34):12194–9.
700 7. Ishino T, Chinzei Y, Yuda M. Two proteins with 6-cys motifs are required for
701 malarial parasites to commit to infection of the hepatocyte. Mol Microbiol.
702 2005;58(5):1264–75.
703 8. van Schaijk BC, Janse CJ, van Gemert GJ, van Dijk MR, Gego A, Franetich

JF, et al. Gene disruption of Plasmodium falciparum p52 results in attenuation of malaria liver stage development in cultured primary human hepatocytes. PLoS One. 2008;3(10):e3549.

9. Kaushansky A, Douglass AN, Arang N, Vigdorovich V, Dambrauskas N, Kain HS, et al. Malaria parasites target the hepatocyte receptor EphA2 for successful host infection. Science. 2015 Nov 27;350(6264):1089–92.

10. Labaied M, Harupa A, Dumpit RF, Coppens I, Mikolajczak SA, Kappe SHI. Plasmodium yoelii sporozoites with simultaneous deletion of P52 and P36 are completely attenuated and confer sterile immunity against infection. Infect Immun. 2007;75(8):3758–68.

11. Bargieri D, Lagal V, Andenmatten N, Tardieux I, Meissner M, Ménard R. Host Cell Invasion by Apicomplexan Parasites: The Junction Conundrum. PLoS Pathog. 2014;10(9):1–9.

12. Pileri P, Uematsu Y, Campagnoli S, Galli G, Falugi F, Petracca R, et al. Binding of hepatitis C virus to CD81. Science. 1998;282(5390):938–41.

13. Silvie O, Rubinstein E, Franetich J-F, Prenant M, Belnoue E, Rénia L, et al. Hepatocyte CD81 is required for Plasmodium falciparum and Plasmodium yoelii sporozoite infectivity. Nat Med. 2003 Jan;9(1):93–6.

14. Silvie O, Greco C, Franetich JF, Dubart-Kupperschmitt A, Hannoun L, van Gemert GJ, et al. Expression of human CD81 differently affects host cell susceptibility to malaria sporozoites depending on the Plasmodium species. Cell Microbiol. 2006;8(7):1134–46.

15. Risco-Castillo V, Topcu S, Son O, Briquet S, Manzoni G, Silvie O. CD81 is required for rhoptry discharge during host cell invasion by Plasmodium yoelii sporozoites. Cell Microbiol. 2014;16(10):1533–48.

16. Silvie O, Charrin S, Billard M, Franetich JF, Clark KL, van Gemert GJ, et al. Cholesterol contributes to the organization of tetraspanin-enriched microdomains and to CD81-dependent infection by malaria sporozoites. J Cell Sci. 2006;119(Pt 10):1992–2002.
17. Charrin S, Yalaoui S, Bartosch B, Cocquerel L, Franetich JF, Boucheix C, et al. The Ig domain protein CD9P-1 down-regulates CD81 ability to support Plasmodium yoelii infection. J Biol Chem. 2009;284(46):31572–8.
18. Silvie O, Franetich JF, Boucheix C, Rubinstein E, Mazier D. Alternative invasion pathways for Plasmodium berghei sporozoites. Int J Parasitol. 2007;37(2):173–82.
19. Yalaoui S, Huby T, Franetich J-F, Gego A, Rametti A, Moreau M, et al. Scavenger receptor BI boosts hepatocyte permissiveness to Plasmodium infection. Cell Host Microbe. 2008 Sep 11;4(3):283–92.
20. Rodrigues CD, Hannus M, Prudêncio M, Martin C, Gonçalves L a, Portugal S, et al. Host scavenger receptor SR-BI plays a dual role in the establishment of malaria parasite liver infection. Cell Host Microbe. 2008 Sep 11;4(3):271–82.
21. Scarselli E, Ansuini H, Cerino R, Roccasecca RM, Acali S, Filocamo G, et al. The human scavenger receptor class B type I is a novel candidate receptor for the hepatitis C virus. EMBO J. 2002 Oct 1;21(19):5017–25.
22. Bartosch B, Vitelli A, Granier C, Goujon C, Dubuisson J, Pascale S, et al. Cell Entry of Hepatitis C Virus Requires a Set of Co-receptors that Include the CD81 Tetraspanin and the SR-B1 Scavenger Receptor. J Biol Chem. 2003;278(43):41624–30.
23. Acton S, Rigotti A, Landschulz KT, Xu S, Hobbs HH, Krieger M. Identification of scavenger receptor SR-BI as a high density lipoprotein receptor. Science. 1996

754 Jan 26;271(5248):518–20.
755 24. Foquet L, Hermsen CC, Verhoye L, van Gemert G-J, Cortese R, Nicosia A, et
756 al. Anti-CD81 but not anti-SR-BI blocks Plasmodium falciparum liver infection
757 in a humanized mouse model. J Antimicrob Chemother. 2015 Feb 4;
758 25. Mazier D, Landau I, Druilhe P, Miltgen F, Guguen-Guillouzo C, Baccam D, et
759 al. Cultivation of the liver forms of Plasmodium vivax in human hepatocytes.
760 Nature. 1984;307(5949):367–9.
761 26. Zahid MN, Turek M, Xiao F, Thi VLD, Guérin M, Fofana I, et al. The
762 postbinding activity of scavenger receptor class B type I mediates initiation of
763 hepatitis C virus infection and viral dissemination. Hepatology. 2013
764 Feb;57(2):492–504.
765 27. Dembele L, Gego A, Zeeman AM, Franetich JF, Silvie O, Rametti A, et al.
766 Towards an in vitro model of Plasmodium hypnozoites suitable for drug
767 discovery. PLoS One. 2011;6(3):e18162.
768 28. Charrin S, Le Naour F, Oualid M, Billard M, Faure G, Hanash SM, et al. The
769 major CD9 and CD81 molecular partner. Identification and characterization of
770 the complexes. J Biol Chem. 2001;276(17):14329–37.
771 29. Berditchevski F, Zutter MM, Hemler ME. Characterization of novel complexes
772 on the cell surface between integrins and proteins with 4 transmembrane
773 domains (TM4 proteins). Mol Biol Cell. 1996 Feb;7(2):193–207.
774 30. Manzoni G, Briquet S, Risco-Castillo V, Gaultier C, Topcu S, Ivanescu ML, et
775 al. A rapid and robust selection procedure for generating drug-selectable
776 marker-free recombinant malaria parasites. Sci Rep. 2014;4:4760.
777 31. Mota MM, Pradel G, Vanderberg JP, Hafalla JC, Frevert U, Nussenzweig RS,
778 et al. Migration of Plasmodium sporozoites through cells before infection.

779 Science. 2001;291(5501):141–4.
780 32. Risco-Castillo V, Topçu S, Marinach C, Manzoni G, Bigorgne AE, Briquet S, et
781 al. Malaria Sporozoites Traverse Host Cells within Transient Vacuoles. Cell
782 Host Microbe. 2015 Oct 21;18(5):593–603.
783 33. VanBuskirk KM, O'Neill MT, De La Vega P, Maier AG, Krzych U, Williams J, et
784 al. Preerythrocytic, live-attenuated Plasmodium falciparum vaccine candidates
785 by design. Proc Natl Acad Sci. 2009 Aug 4;106(31):13004–9.
786 34. Mikolajczak SA, Lakshmanan V, Fishbaugher M, Camargo N, Harupa A,
787 Kaushansky A, et al. A Next-generation Genetically Attenuated Plasmodium
788 falciparum Parasite Created by Triple Gene Deletion. Mol Ther. 2014
789 Sep;22(9):1707–15.
790 35. Mueller AK, Camargo N, Kaiser K, Andorfer C, Frevert U, Matuschewski K, et
791 al. Plasmodium liver stage developmental arrest by depletion of a protein at the
792 parasite-host interface. Proc Natl Acad Sci U S A. 2005;102(8):3022–7.
793 36. Iwanaga S, Khan SM, Kaneko I, Christodoulou Z, Newbold C, Yuda M, et al.
794 Functional identification of the Plasmodium centromere and generation of a
795 Plasmodium artificial chromosome. Cell Host Microbe. 2010;7(3):245–55.
796 37. Kapadia SB, Barth H, Baumert T, McKeating J a, Chisari F V. Initiation of
797 hepatitis C virus infection is dependent on cholesterol and cooperativity
798 between CD81 and scavenger receptor B type I. J Virol. 2007;81(1):374–83.
799 38. Colpitts CC, Baumert TF. Hepatitis C virus cell entry: a target for novel antiviral
800 strategies to address limitations of direct acting antivirals. Hepatol Int. 2016
801 Sep 5;10(5):741–8.
802 39. Evans MJ, von Hahn T, Tscherne DM, Syder AJ, Panis M, Wölk B, et al.
803 Claudin-1 is a hepatitis C virus co-receptor required for a late step in entry.

804 Nature. 2007;446(7137):801–5.
805 40. Ploss A, Evans MJ, Gaysinskaya V a, Panis M, You H, de Jong YP, et al.
806 Human occludin is a hepatitis C virus entry factor required for infection of
807 mouse cells. Nature. 2009 Feb 12;457(7231):882–6.
808 41. Charrin S, Jouannet S, Boucheix C, Rubinstein E. Tetraspanins at a glance. J
809 Cell Sci. 2014;127(Pt 17):3641–8.
810 42. Charrin S, le Naour F, Silvie O, Milhiet PE, Boucheix C, Rubinstein E. Lateral
811 organization of membrane proteins: tetraspanins spin their web. Biochem J.
812 2009;420(2):133–54.
813 43. Neculai D, Schwake M, Ravichandran M, Zunke F, Collins RF, Peters J, et al.
814 Structure of LIMP-2 provides functional insights with implications for SR-BI and
815 CD36. Nature. Nature Publishing Group; 2013;504(7478):172–6.
816 44. Baruch DI, Gormely JA, Ma C, Howard RJ, Pasloske BL. Plasmodium
817 falciparum erythrocyte membrane protein 1 is a parasitized erythrocyte
818 receptor for adherence to CD36, thrombospondin, and intercellular adhesion
819 molecule 1. Proc Natl Acad Sci U S A. 1996 Apr 16;93(8):3497–502.
820 45. Oquendo P, Hundt E, Lawler J, Seed B. CD36 directly mediates cytoadherence
821 of Plasmodium falciparum parasitized erythrocytes. Cell. 1989 Jul 14;58(1):95–
822 101.
823 46. Barnwell JW, Asch AS, Nachman RL, Yamaya M, Aikawa M, Ingravallo P. A
824 human 88-kD membrane glycoprotein (CD36) functions in vitro as a receptor
825 for a cytoadherence ligand on Plasmodium falciparum-infected erythrocytes. J
826 Clin Invest. 1989 Sep;84(3):765–72.
827 47. Ockenhouse CF, Klotz FW, Tandon NN, Jamieson GA. Sequestrin, a CD36
828 recognition protein on Plasmodium falciparum malaria-infected erythrocytes

identified by anti-idiotype antibodies. Proc Natl Acad Sci U S A. 1991 Apr 15;88(8):3175–9.

48. Orito Y, Ishino T, Iwanaga S, Kaneko I, Kato T, Menard R, et al. Liver-specific protein 2: a Plasmodium protein exported to the hepatocyte cytoplasm and required for merozoite formation. Mol Microbiol. 2013 Jan;87(1):66–79.

49. Annoura T, Van Schaijk BCL, Ploemen IHJ, Sajid M, Lin JW, Vos MW, et al. Two Plasmodium 6-Cys family-related proteins have distinct and critical roles in liver-stage development. FASEB J. 2014;28:2158–70.

50. Franke-Fayard B, Janse CJ, Cunha-Rodrigues M, Ramesar J, Buscher P, Que I, et al. Murine malaria parasite sequestration: CD36 is the major receptor, but cerebral pathology is unlinked to sequestration. Proc Natl Acad Sci U S A. 2005;102(32):11468–73.

51. Sinnis P, Febbraio M. Plasmodium yoelii sporozoites infect CD36-deficient mice. Exp Parasitol. 2002;100(1):12–6.

52. Tonkin ML, Arredondo S a, Loveless BC, Serpa JJ, Makepeace K a T, Sundar N, et al. Structural and biochemical characterization of Plasmodium falciparum 12 (Pf12) reveals a unique interdomain organization and the potential for an antiparallel arrangement with Pf41. J Biol Chem. 2013 May 3;288(18):12805–17.

53. Taechalertpaisarn T, Crosnier C, Bartholdson SJ, Hodder AN, Thompson J, Bustamante LY, et al. Biochemical and functional analysis of two Plasmodium falciparum blood-stage 6-cys proteins: P12 and P41. PLoS One. 2012 Jan;7(7):e41937.

54. Parker ML, Peng F, Boulanger MJ. The Structure of Plasmodium falciparum Blood-Stage 6-Cys Protein Pf41 Reveals an Unexpected Intra-Domain

Insertion Required for Pf12 Coordination. PLoS One. 2015 Jan;10(9):e0139407.

55. Lindner SE, Swearingen KE, Harupa A, Vaughan AM, Sinnis P, Moritz RL, et al. Total and putative surface proteomics of malaria parasite salivary gland sporozoites. Mol Cell Proteomics. 2013;12(5):1127–43.

56. Swearingen KE, Lindner SE, Shi L, Shears MJ, Harupa A, Hopp CS, et al. Interrogating the Plasmodium Sporozoite Surface: Identification of Surface-Exposed Proteins and Demonstration of Glycosylation on CSP and TRAP by Mass Spectrometry-Based Proteomics. Yates J, editor. PLOS Pathog. 2016 Apr 29;12(4):e1005606.

57. van Dijk MR, van Schaijk BCL, Khan SM, van Dooren MW, Ramesar J, Kaczanowski S, et al. Three members of the 6-cys protein family of Plasmodium play a role in gamete fertility. PLoS Pathog. 2010 Apr;6(4):e1000853.

58. Rosa TFA, Flammersfeld A, Ngwa CJ, Kiesow M, Fischer R, Zipfel PF, et al. The Plasmodium falciparum blood stages acquire factor H family proteins to evade destruction by human complement. Cell Microbiol. 2016 Apr;18(4):573–90.

59. Kennedy AT, Schmidt CQ, Thompson JK, Weiss GE, Taechalertpaisarn T, Gilson PR, et al. Recruitment of Factor H as a Novel Complement Evasion Strategy for Blood-Stage Plasmodium falciparum Infection. J Immunol. 2016 Feb 1;196(3):1239–48.

60. Molina-Cruz A, Garver LS, Alabaster A, Bangiolo L, Haile A, Winikor J, et al. The human malaria parasite Pfs47 gene mediates evasion of the mosquito immune system. Science. 2013 May 24;340(6135):984–7.

879 61. Ramphul UN, Garver LS, Molina-Cruz A, Canepa GE, Barillas-Mury C.
880 Plasmodium falciparum evades mosquito immunity by disrupting JNK-mediated
881 apoptosis of invaded midgut cells. Proc Natl Acad Sci U S A. 2015 Feb
882 3;112(5):1273–80.
883 62. Molina-Cruz A, Canepa GE, Kamath N, Pavlovic N V, Mu J, Ramphul UN, et al.
884 Plasmodium evasion of mosquito immunity and global malaria transmission:
885 The lock-and-key theory. Proc Natl Acad Sci U S A. 2015 Nov
886 23;112(49):15178–83.
887 63. Besteiro S, Dubremetz JF, Lebrun M. The moving junction of apicomplexan
888 parasites: a key structure for invasion. Cell Microbiol. 2011;13(6):797–805.
889 64. Naudin C, Sirvent A, Leroy C, Larive R, Simon V, Pannequin J, et al. SLAP
890 displays tumour suppressor functions in colorectal cancer via destabilization of
891 the SRC substrate EPHA2. Nat Commun. 2014 Jan;5:3159f.
892 65. Mineo C, Shaul PW. HDL stimulation of endothelial nitric oxide synthase: a
893 novel mechanism of HDL action. Trends Cardiovasc Med. 2003
894 Aug;13(6):226–31.
895 66. Felmlee DJ, Coilly A, Chung RT, Samuel D, Baumert TF. New perspectives for
896 preventing hepatitis C virus liver graft infection. The Lancet Infectious
897 Diseases. 2016. p. 735–45.
898 67. Andolina C, Landier J, Carrara V, Chu CS, Franetich J-F, Roth A, et al. The
899 suitability of laboratory-bred Anopheles cracens for the production of
900 Plasmodium vivax sporozoites. Malar J. 2015 Jan;14:312.
901 68. Tsuji M, Mattei D, Nussenzweig RS, Eichinger D, Zavala F. Demonstration of
902 heat-shock protein 70 in the sporozoite stage of malaria parasites. Parasitol
903 Res. 1994;80(1):16–21.

904 69. Prudêncio M, Rodrigues CD, Ataíde R, Mota MM. Dissecting in vitro host cell
905 infection by Plasmodium sporozoites using flow cytometry. Cell Microbiol. 2008
906 Jan;10(1):218–24.
907 70. Maillard P, Huby T, Andréo U, Moreau M, Chapman J, Budkowska A. The
908 interaction of natural hepatitis C virus with human scavenger receptor SR-
909 BI/Cla1 is mediated by ApoB-containing lipoproteins. FASEB J. 2006
910 Apr;20(6):735–7.
911 71. Zeisel MB, Koutsoudakis G, Schnober EK, Haberstroh A, Blum HE, Cosset F-
912 L, et al. Scavenger receptor class B type I is a key host factor for hepatitis C
913 virus infection required for an entry step closely linked to CD81. Hepatology.
914 2007 Dec;46(6):1722–31.
915 72. Yalaoui S, Zougbede S, Charrin S, Silvie O, Arduise C, Farhati K, et al.
916 Hepatocyte permissiveness to Plasmodium infection is conveyed by a short
917 and structurally conserved region of the CD81 large extracellular domain. PLoS
918 Pathog. 2008;4(2):e1000010.
919 73. Janse CJ, Ramesar J, Waters AP. High-efficiency transfection and drug
920 selection of genetically transformed blood stages of the rodent malaria parasite
921 Plasmodium berghei. Nat Protoc. 2006;1(1):346–56.
922 74. Yang J, Yan R, Roy A, Xu D, Poisson J, Zhang Y. The I-TASSER Suite: protein
923 structure and function prediction. Nat Methods. 2015 Jan;12(1):7–8.
924 75. Emsley P, Cowtan K. Coot: model-building tools for molecular graphics. Acta
925 Crystallogr D Biol Crystallogr. 2004 Dec;60(Pt 12 Pt 1):2126–32.
926
927
928

FIGURE LEGENDS

Figure 1. Anti-SR-BI antibodies inhibit *P. vivax* but not *P. falciparum* sporozoite infection. A. Primary human hepatocyte cultures were incubated with *P. vivax* sporozoites in the presence of anti-CD81 and/or anti-SR-BI mAbs at 20 µg/ml, and the number of EEF-infected cells was determined 5 days post-infection after labeling of the parasites with anti-HSP70 antibodies. **B**. Primary human hepatocytes were incubated with *P. vivax* sporozoites in the presence or absence of anti-SR-BI polyclonal rabbit serum (diluted 1/100), and the number of EEFs was determined at day 5 as by immunofluorescence. **C**. Primary human hepatocyte cultures were incubated with *P. falciparum* sporozoites in the presence of anti-CD81 mAb (20 µg/ml) and/or anti-SR-BI polyclonal rabbit serum (diluted 1/100), and the number of EEF-infected cells was determined 5 days post-infection after labeling of the parasites with anti-HSP70 antibodies. Results from 3 independent experiments are shown and expressed as the percentage of control (mean +/- SD). **D**. Immunofluorescence analysis of *P. vivax* EEFs at day 5 post-infection of primary human hepatocytes. Parasites were labeled with anti-HSP70 antibodies (green), and nuclei were stained with Hoechst 33342 (blue). Large EEFs and small EEFs were observed in both control and anti-SR-BI antibody-treated cultures. Scale bars, 10 µm. **E**. Inhibitory activity of anti-SR-BI antibodies on small EEFs (white histograms) and large EEFs (black histograms). The results from 4 independent experiments are shown, and are expressed as the percentage of inhibition observed with anti-SR-BI antibodies as compared to the control.

Figure 2. Infection of human HepG2 cells by *P. berghei* sporozoites depends on SR-BI. **A**. HepG2 cells were incubated with *P. berghei* sporozoites for 3 h in the absence (Control) or presence of increasing concentrations of rabbit polyclonal SR-BI antisera. Infected cultures were further incubated for 24h before quantification of EEFs-infected cells by fluorescence microscopy. **B**. HepG2 cell cultures were infected with PbGFP sporozoites as in A, and the number of invaded cells (GFP+) was quantified by FACS 3 hours post-infection.

C. HepG2 cells were incubated for 3 hours with PbGFP sporozoites and rhodamine-labeled dextran, in the presence or absence of anti-SR-BI antibodies. The percentage of traversed (dextran-positive) cells was then determined by FACS. **D**. HepG2 cells transfected with siRNA oligonucleotides targeting SR-BI (siSR-BI, red histogram) or with a control siRNA (siCont, blue histogram) were stained with anti-SR-BI antibodies and analyzed by flow cytometry. The negative staining control is in grey. **E**. *P. berghei* EEF number in HepG2 cells transfected with siRNA oligonucleotides targeting SR-BI (siSR-BI) or a control siRNA (siCont). **F**. HepG2 cells transfected with siRNA oligonucleotides targeting SR-BI (siSR-BI) or a control siRNA (siCont) were infected with PbGFP sporozoites and incubated for 24 hours, before measurement of the mean fluorescence intensity (GFP MFI) of infected (GFP-positive) cells by FACS.

Figure 3. CD81 and SR-BI define alternative entry routes for *P. berghei* sporozoites. A. HepG2/CD81 cells were incubated with *P. berghei* sporozoites in the presence or absence of anti-human CD81 and/or SR-BI mAbs, and the number of EEFs-infected cells was determined by fluorescence microscopy 24 hours post-infection. **B**. *P. berghei* EEF numbers in HepG2/CD81 cells transfected with siRNA oligonucleotides targeting CD81 (siCD81) and/or SR-BI (siSR-BI). **C**. HepG2/CD81 cells were incubated with *Pb*GFP sporozoites for 15-120 min, in the presence or absence of anti-CD81 and/or anti-SR-BI antibodies, then trypsinized and directly analyzed by FACS to quantify invaded (GFP-positive) cells. **D**. Protein extracts from Hepa1-6 cells and Hepa1-6 cells transiently transfected with a human SR-BI expression plasmid were analyzed by Western blot using antibodies recognizing mouse and human SR-BI (Abcam) or mouse CD81 (MT81). **E**. Hepa1-6 cells were transfected first with siRNA oligonucleotides targeting endogenous mouse CD81 (simCD81), then with plasmids encoding human CD81 (hCD81) or SR-BI (hSR-BI). Cells were then incubated with PbGFP sporozoites, and the number of infected (GFP-positive) cells was determined 24h post-infection by FACS.

Figure 4. Infection of HepG2/CD81 cells by *P. yoelii* sporozoites depends on CD81 but not SR-BI. A. HepG2/CD81 cells were incubated with *P. yoelii* sporozoites in the presence of anti-CD81 mAb (20 µg/ml) or anti-SR-BI polyclonal rabbit serum (diluted 1/100), and the number of EEF-infected cells was determined 24 hours post-infection by fluorescence microscopy. Results from 3 independent experiments are shown and expressed as the percentage of control (mean +/- SD). **B**. *P. yoelii* EEF numbers in HepG2/CD81 cells transfected with siRNA oligonucleotides targeting CD81 (siCD81) and/or SR-BI (siSR-BI).

Figure 5. The 6-cys proteins P52 and P36 are required for productive host cell invasion. A-B. HepG2 (A) or Hepa1-6 cells (B) were incubated with PbGFP (blue lines) or Pb*Δp52/p36* sporozoites (red lines) for 15-120 minutes, in the presence (dotted lines) or absence (solid lines) of anti-SR-BI (A) or anti-CD81 (B) antibodies. Cells were then trypsinized and directly analyzed by FACS to quantify invaded (GFP-positive) cells. **C**. HepG2 and HepG2/CD81 cells were infected with PbGFP or Pb*Δp52/p36* sporozoites and the number of EEFs was determined 28 hours post-infection by fluorescence microscopy. **D**. HepG2 and HepG2/CD81 cells infected with PbGFP or Pb*Δp52/p36* sporozoites were fixed at 28 hours post-infection, stained with anti-UIS4 antibodies (red) and the nuclear stain Hoechst 33342 (blue), and examined by fluorescence microscopy. Parasites were detected based on GFP expression (green). Scale bars, 10 µm. **E**. Quantification of UIS4 expression in HepG2 and HepG2/CD81 cells infected with PbGFP (red) or Pb*Δp52/p36* (black). **F**. HepG2 (dotted lines) and HepG2/CD81 cells (solid lines) were incubated with PyGFP (blue lines) or Py*Δp52/p36* sporozoites (red lines) for 15-180 minutes, trypsinized, and directly analyzed by FACS to quantify invaded (GFP-positive) cells. **G**. HepG2/CD81 cells were infected with PyGFP or Py*Δp52/p36* sporozoites and the number of EEFs was determined 24 hours post-infection by fluorescence microscopy. **H**. HepG2 and HepG2/CD81 cells infected with PyGFP or Py*Δp52/p36* sporozoites were fixed at 24 hours post-infection, stained with anti-UIS4 antibodies (red) and the nuclear stain Hoechst 33342 (blue), and examined by fluorescence microscopy. Parasites were detected based on GFP expression (green). Scale

bars, 10 µm. **I**. Quantification of UIS4 expression in HepG2 and HepG2/CD81 cells infected with PyGFP (red) or PyΔ*p52/p36* (black).

Figure 6. P36 mediates CD81-independent entry in *P. berghei* sporozoites. A. HepG2 (blue histograms) or HepG2/CD81 cells (red histograms) were incubated with sporozoites from PbΔ*p52/p36* parasites genetically complemented with *P. berghei* and/or *P. yoelii* P52 and P36, and analysed by FACS or fluorescence microscopy to determine the number of GFP-positive cells 24h post-infection. Results from 3 independent experiments are shown and are expressed as the percentage of infection in comparison to control PbGFP-infected cultures (mean +/-SD). **B**. Immunofluorescence analysis of UIS4 expression in HepG2 or HepG2/CD81 cells infected with genetically complemented PbΔ*p52/p36* sporozoites. Cells were fixed with PFA 28 hours post-infection, permeabilized, and stained with anti-UIS4 antibodies (red) and the nuclear stain Hoechst 33342 (blue). Parasites were detected based on GFP expression (green). Scale bars, 10 µm. **C-D**. HepG2/CD81 (C) and HepG2 (D) cells were infected with PbGFP, PbΔ*p52/p36* and complemented PbΔ*p52/p36* sporozoites. The numbers of UIS4-positive (red histograms) and UIS4-negative (black histograms) EEFs were determined by fluorescence microscopy 24 hours post-infection.

Figure 7. Transgenic *P. yoelii* sporozoites expressing *Pb*P36 can infect CD81-null cells via SR-BI A. HepG2 (blue) and HepG2/CD81 cells (red) were incubated with genetically complemented PyΔ*p52/p36* sporozoites, and fixed 24h post-infection. The number of UIS4-positive vacuoles was then determined by immunofluorescence. **B**. Immunofluorescence analysis of UIS4 expression in HepG2 or HepG2/CD81 cells infected with sporozoites of PyΔ*p52/p36* parasites genetically complemented with P52 and P36 from *P. berghei* or *P. yoelii*. Cells were fixed with PFA, permeabilized, and stained with anti-UIS4 antibodies (red) and the nuclear stain Hoechst 33342 (blue). Parasites were detected based on GFP expression (green). Scale bars, 10 µm. **C**. Quantification of UIS4 expression in HepG2 (blue) and HepG2/CD81 cells (red) infected with genetically complemented PyΔ*p52/p36*

sporozoites and processed as in B for immunofluorescence. **D**. HepG2 cells were incubated with Py*Δp52/p36* sporozoites complemented with PbP36 and either PbP52 or PyP52, in the presence or absence of anti-SR-BI antibodies. Infected cultures were fixed 24h post-infection, and the number of EEFs was then determined by fluorescence microscopy.

Figure 8. Model of host cell entry pathways for *Plasmodium* sporozoites. A. Host cell membrane proteins CD81 and SR-BI define two independent entry routes for *Plasmodium* sporozoites. *P. falciparum* and *P. yoelii* sporozoites require CD81 for infection, whereas *P. vivax* sporozoites infect hepatocytes using SR-BI. *P. berghei* sporozoites can enter cells alternatively via CD81 or SR-BI. **B**. The 6-cysteine domain protein P36 determines host cell receptor usage during *P. yoelii* and *P. berghei* sporozoite invasion. Whilst PyP36 supports only CD81-dependent sporozoite entry, PbP36 mediates sporozoite invasion through both CD81- and SR-BI-dependent pathways. **C**. Model of the 3D structure of *P. berghei* P36, established based on the crystal structure of PfP12 (2YMO). In the ribbon diagram, the tandem 6-cysteine domains are shown in blue (D1) and green (D2), respectively, and the cysteine residues and disulphide bonds in yellow. The loop located between the third and fourth cysteine residues of the D2 domain (inter-cys loop) is indicated in red.

SUPPLEMENTAL FIGURE LEGENDS

Figure 2-figure supplement 1. CD81 and SR-BI surface expression in HepG2 and HepG2/CD81 cells. HepG2 (A) and HepG2/CD81 cells (B) were stained with anti-CD81 (red histograms) or anti-SR-BI (green histograms) antibodies and analyzed by FACS.

Figure 2-figure supplement 2. Anti-SR-BI antibodies neutralize *P. berghei* infection of HepG2 cells. Effect of anti-SR-BI rat polyclonal antibodies (pAb) and mouse mAb on *P. berghei* EEF numbers in HepG2 cells.

Figure 2-figure supplement 3. Effect of SR-BI silencing on sporozoite cell traversal and invasion. HepG2 cells transfected with siRNA oligonucleotides targeting SR-BI (siSR-BI) or a control siRNA (siCont) were incubated for 3 hours with PbGFP sporozoites and rhodamine-labeled dextran, and the percentage of invaded cells (GFP-positive, green bars) and traversed cells (dextran-positive, red bars) was determined by FACS.

Figure 3-figure supplement 1. Effect of anti-CD81 and anti-SR-BI antibodies on *P. berghei* sporozoite cell traversal and intracellular development. A. HepG2/CD81 cells were incubated for 3 hours with PbGFP sporozoites and rhodamine-labeled dextran, in the presence or absence of anti-CD81 and/or SR-BI antibodies. The percentage of traversed (dextran-positive) cells was then determined by FACS. **B**. HepG2/CD81 cells were infected with PbGFP sporozoites in the presence or absence of anti-CD81 or anti-SR-BI antibodies, and incubated for 24 hours before measurement of the MFI of infected (GFP-positive) cells by FACS.

Figure 5-figure supplement 1. Targeted gene deletion of p52 and p36 in *P. berghei*. A. Replacement strategy to generate PbΔ*p52p36* parasites. The wild-type (WT) genomic locus of *P. berghei* p52/p36 was targeted with a GOMO-GFP replacement plasmid containing a 5’

and a 3' homologous sequence inserted on each side of the plasmid GFP/hDHFR-yFCU/mCherry triple cassette. Upon double crossover recombination, the adjacent *p52* and *p36* genes are replaced by the plasmid cassettes. Subsequent recombination between the two identical PbDHFR/TS 3' UTR sequences (pink lollipops) results in excision of hDHFR-yFCU and mCherry. Genotyping primers and expected PCR fragments are indicated by arrows and lines, respectively. **B-C**. PCR analysis of genomic DNA isolated from control PbGFP and Pb*Δp52p36* parasites recovered after positive selection with pyrimethamine (B) and after negative selection with 5-fluorocytosine (C). Confirmation of the predicted recombination events was achieved with primer combinations specific for 5' integration (5' integr.), 3' integration (3' integr.) or 3' integration followed by marker excision (3' excised). Primers used for genotyping are indicated in the Materials and Methods. The absence of amplification with primer combinations specific for the WT locus (WT) and the non-excised integrated construct (3' integration) confirms that the final populations contain only Pb*Δp52p36* drug-selectable marker-free *P. berghei* parasites.

Figure 5-figure supplement 2. Targeted gene deletion of p52 and p36 in *P. yoelii*. A. Replacement strategy to generate Py*Δp52p36* parasites. The wild-type (WT) genomic locus of *P. yoelii* p52/p36 in the PyGFP parental line was targeted with a GOMO replacement plasmid containing a 5' and a 3' homologous sequence from *pyp52* inserted on each side of a hDHFR-yFCU/mCherry double cassette. An additional 3' homologous sequence from *pyp36* (36-3') was inserted immediately downstream of the 5' homologous sequence from *pyp52* (52-5'). Upon double crossover recombination, *pyp52* is replaced by the plasmid cassettes. Subsequent recombination between the two identical 36-3' sequences results in excision of hDHFR-yFCU, mCherry and *pyp36*. Genotyping primers and expected PCR fragments are indicated by arrows and lines, respectively. **B-C**. PCR analysis of genomic DNA isolated from parental PyGFP and Py*Δp52p36* parasites recovered after positive selection with pyrimethamine (B) and after negative selection with 5-fluorocytosine (C). Confirmation of the predicted recombination events was achieved with primer combinations

specific for 5' integration (5' integr.), 3' integration (3' integr.) or 3' integration followed by marker excision (3' excised). Primers used for genotyping are indicated in Materials and methods. The absence of amplification with primer combinations specific for the WT locus (WT) and the non-excised integrated construct (3' integration) confirms that the final populations contain only Py∆*p52p36* drug-selectable marker-free *P. yoelii* parasites.

Figure 5-figure supplement 3. Targeted gene deletion of *p36* in *P. berghei*. A. Replacement strategy to generate Pb∆*p36* parasites. The wild-type (WT) genomic locus of *P. berghei p36* was targeted with a GOMO-GFP replacement plasmid containing a 5' and a 3' homologous sequence inserted on each side of the plasmid GFP/hDHFR-yFCU/mCherry triple cassette. Upon double crossover recombination, the *p36* gene is replaced by the plasmid cassettes. Subsequent recombination between the two identical PbDHFR/TS 3' UTR sequences (pink lollipops) results in excision of hDHFR-yFCU and mCherry. Genotyping primers and expected PCR fragments are indicated by arrows and lines, respectively. **B-C**. PCR analysis of genomic DNA isolated from control PbGFP and Pb∆*p36* parasites recovered after positive selection with pyrimethamine (B) and after negative selection with 5-fluorocytosine (C). Confirmation of the predicted recombination events was achieved with primer combinations specific for 5' integration (5' integr.), 3' integration (3' integr.) or 3' integration followed by marker excision (3' excised). Primers used for genotyping are indicated in the Materials and methods. The absence of amplification with primer combinations specific for the WT locus (WT) and the non-excised integrated construct (3' integration) confirms that the final populations contain only Pb∆*p36* drug-selectable marker-free *P. berghei* parasites.

Figure 5-figure supplement 4. P36 is required for *P. berghei* sporozoite entry via both SR-BI- and CD81-dependent routes. HepG2 and HepG2/CD81 cells were incubated with PbGFP or Pb∆*p36* sporozoites in the presence or absence of anti-CD81 and anti-SR-BI

antibodies, and the percentage of infected (GFP-positive) cells was determined 24 hours post-infection by FACS.

Figure 6-figure supplement 1. Genetic complementation with *p52* and *p36* from *P. falciparum* or *P. vivax* does not restore sporozoite infectivity in PbΔ*p52p36* parasites. **A.** HepG2 and HepG2/CD81 cells were incubated with PbGFP, PbΔ*p52p36* and PbΔ*p52p36* complemented with *p52* and *p36* from *P. falciparum* or *P. vivax*. The percentage of infected (GFP-positive) cells 24 hours post-infection was determined by FACS. **B.** Primary human hepatocytes were incubated with PbGFP, PbΔ*p52p36* and PbΔ*p52p36* complemented with *p52* and *p36* from *P. falciparum* or *P. vivax*. The number of EEFs was determined 24 hours post-infection by fluorescence microscopy.

Figure 8-figure supplement 1. P36 protein sequence analysis. A. Alignment of *P. berghei* and *P. yoelii* P36 protein sequences. Identical, similar and different amino acids are shaded in black, grey and red, respectively. The tandem 6-cys domains D1 and D2 are indicated with blue and green lines, respectively, above the protein sequences. The six cysteine residues of each domain are indicated below the protein sequences. **B**. Schematic representation of the tandem D1 and D2 6-cys domains of P36, showing the disulfide bond arrangement. The position of the “inter-cys loop”, located between the third and fourth cysteine residues of D2, is indicated as a red line. **C**. Alignment of *P. falciparum*, *P. vivax*, *P. berghei* and *P. yoelii* inter-cys loop sequences. Identical and similar amino acids are shaded in black and grey, respectively.

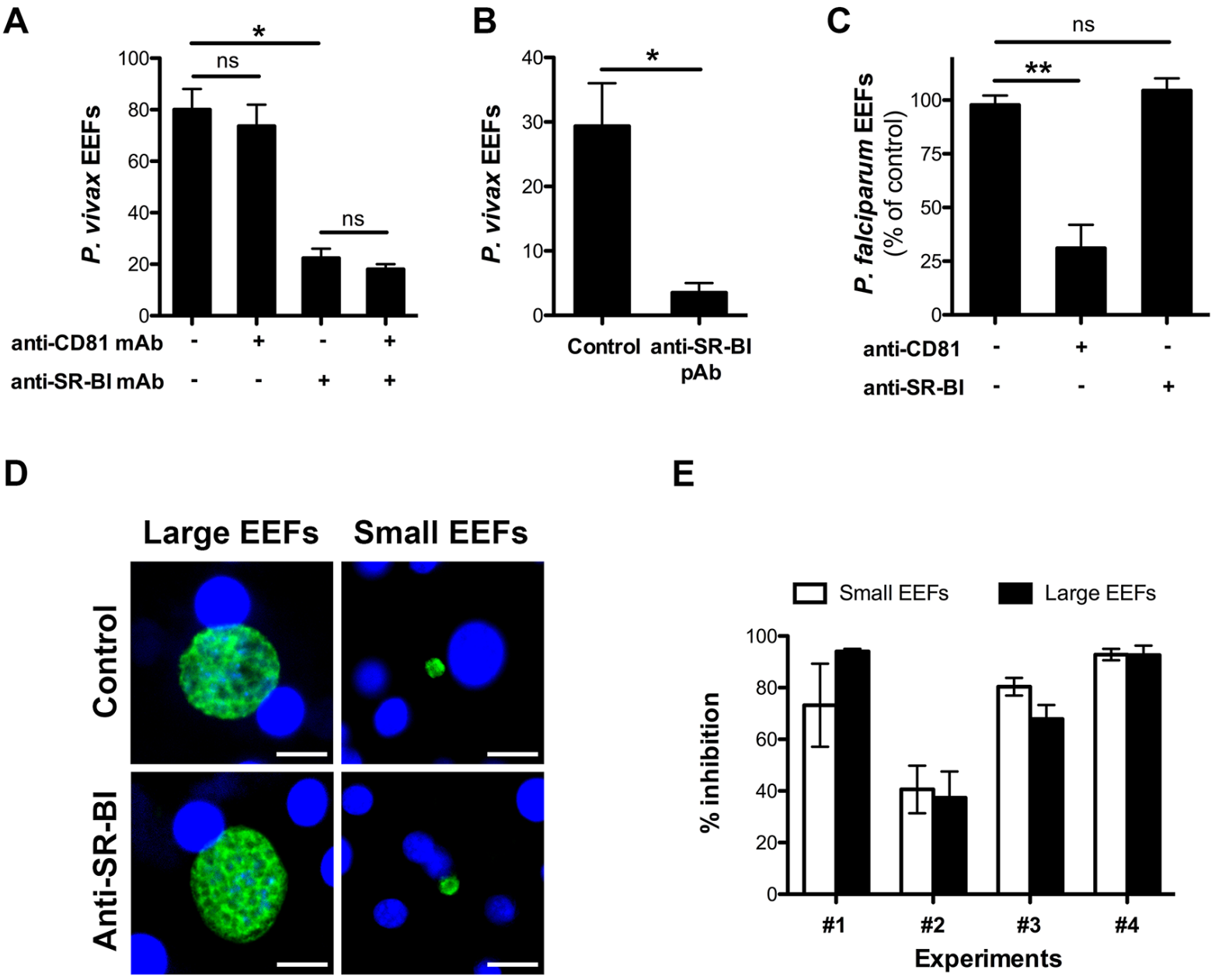
A
*
ns
ns
100
80
60
40
20
0
P. vivax EEFs
anti-CD81 mAb - + - +
anti-SR-BI mAb - - + +
B
*
40
30
20
10
0
P. vivax EEFs
Control
anti-SR-BI pAb
C
ns
**
100
75
50
25
0
P. falciparum EEFs (% of control)
anti-CD81 - + -
anti-SR-BI - - +
D
Large EEFs
Small EEFs
Control
Anti-SR-BI
E
Small EEFs
Large EEFs
100
80
60
40
20
0
% inhibition
#1
#2
#3
#4
Experiments

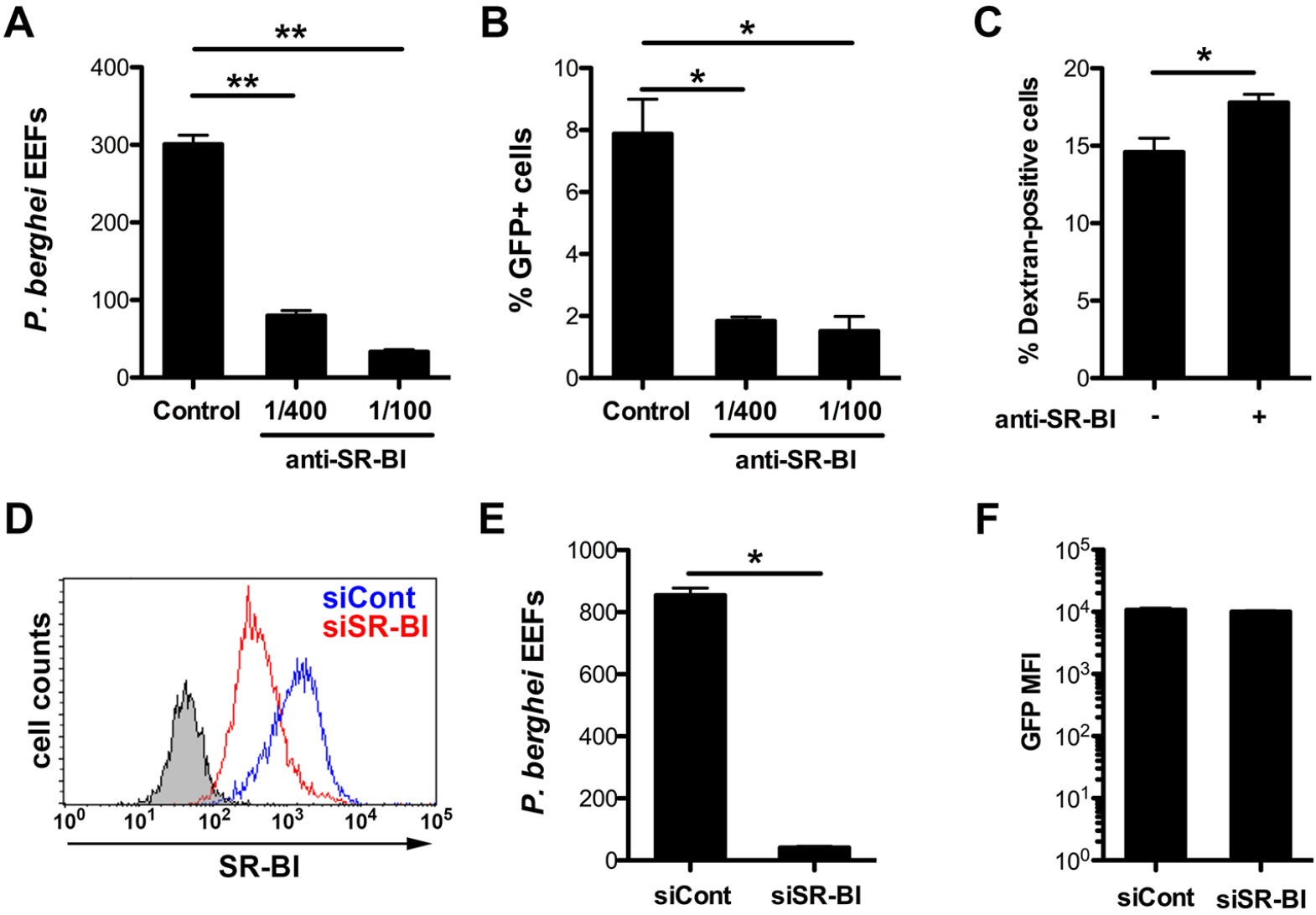
A
B
C
D
E
F
P. berghei EEFs
% GFP+ cells
% Dextran-positive cells
Control
1/400
1/100
anti-SR-BI
anti-SR-BI
-
+
cell counts
siCont
siSR-BI
SR-BI
GFP MFI
siCont
siSR-BI

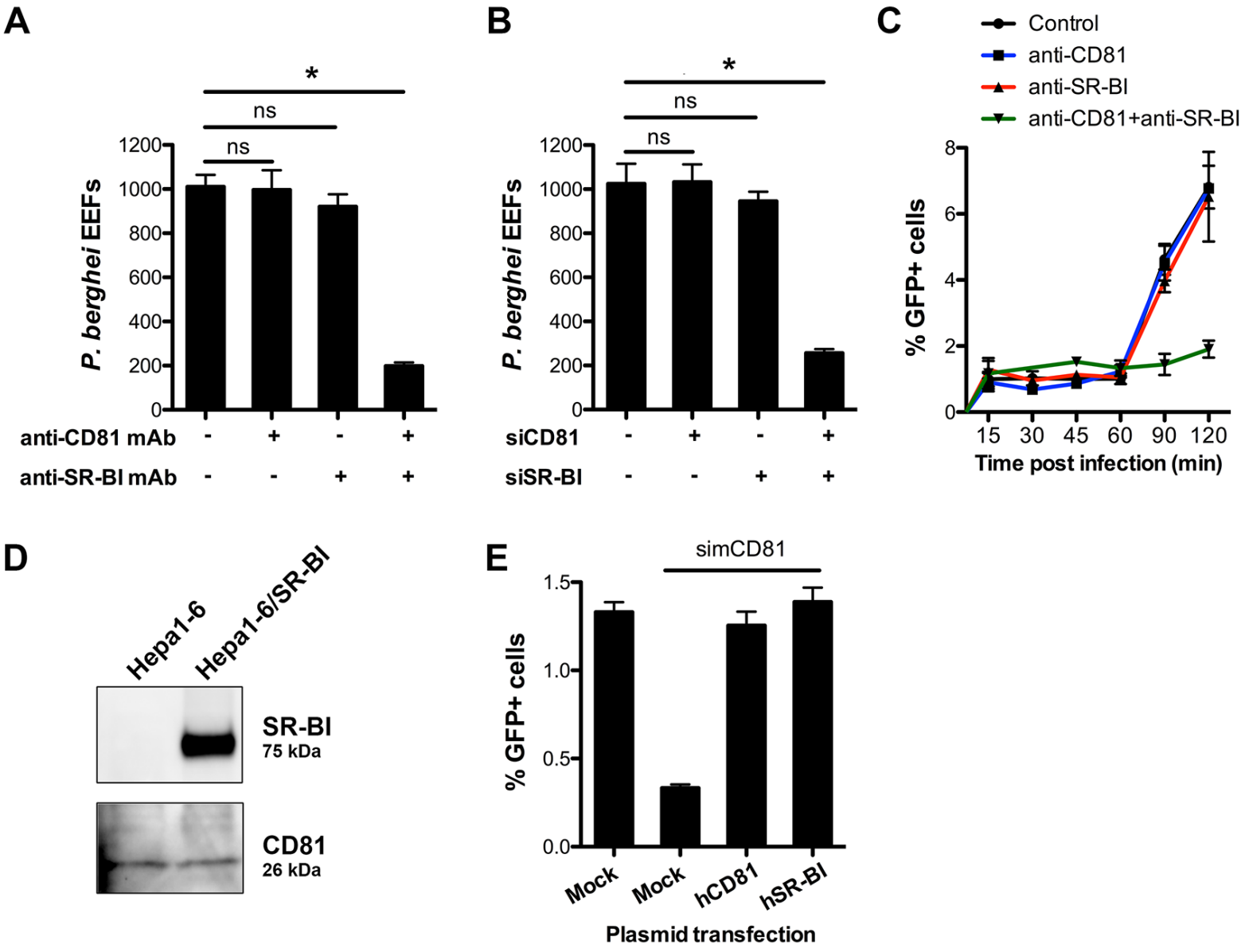
A
*
ns
ns
1200
1000
800
600
400
200
0
P. berghei EEFs
anti-CD81 mAb - + - +
anti-SR-BI mAb - - + +
B
*
ns
ns
1200
1000
800
600
400
200
0
P. berghei EEFs
siCD81 - + - +
siSR-BI - - + +
C
Control
anti-CD81
anti-SR-BI
anti-CD81+anti-SR-BI
8
6
4
2
0
% GFP+ cells
15 30 45 60 90 120
Time post infection (min)
D
Hepa1-6
Hepa1-6/SR-BI
SR-BI
75 kDa
CD81
26 kDa
E
simCD81
1.5
1.0
0.5
0.0
% GFP+ cells
Mock
Mock
hCD81
hSR-BI
Plasmid transfection

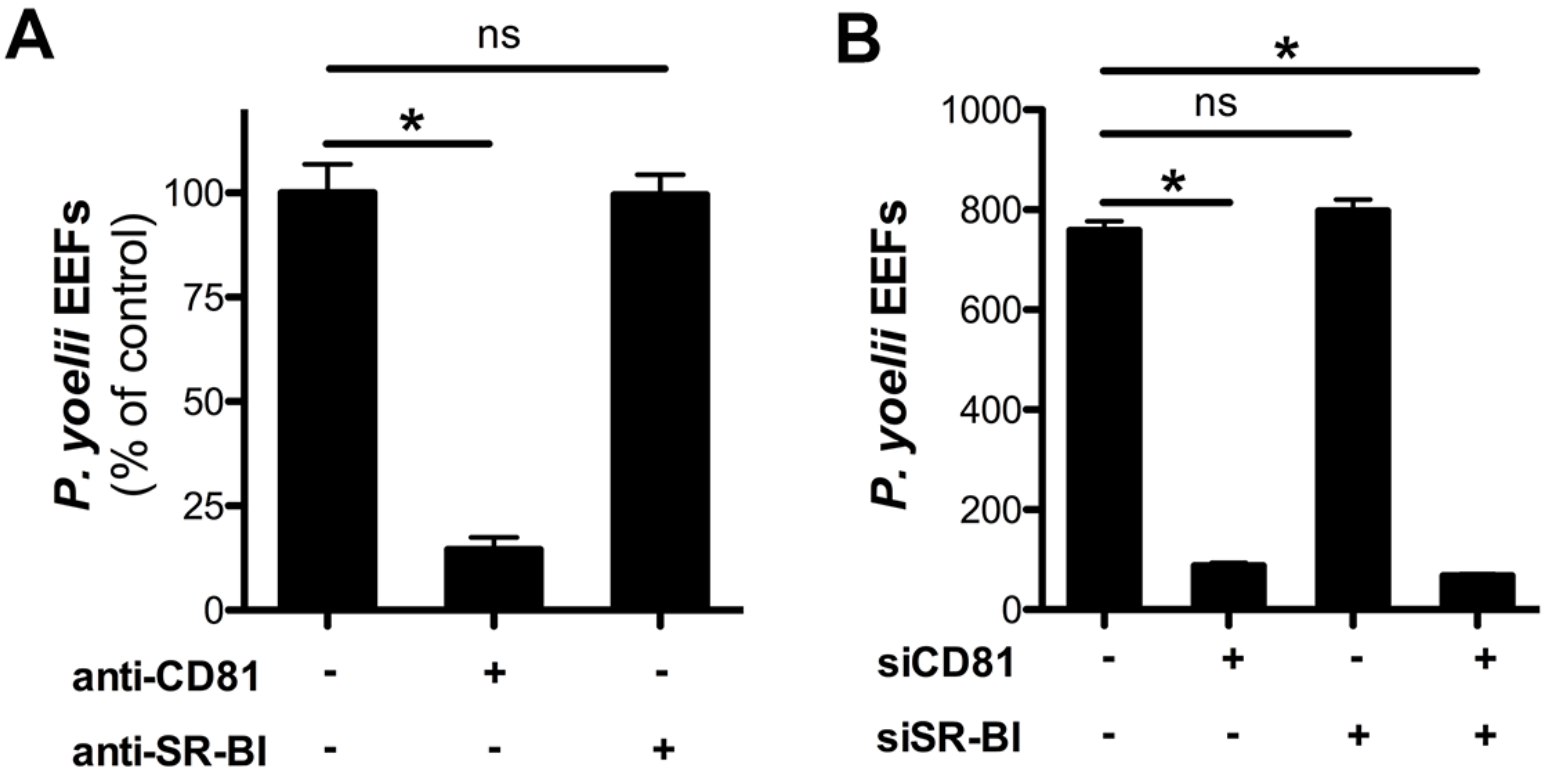
A
ns
*
P. yoelii EEFs
(% of control)
100
75
50
25
0
anti-CD81 - + -
anti-SR-BI - - +
B
*
ns
*
1000
800
600
400
200
0
P. yoelii EEFs
siCD81 - + - +
siSR-BI - - + +

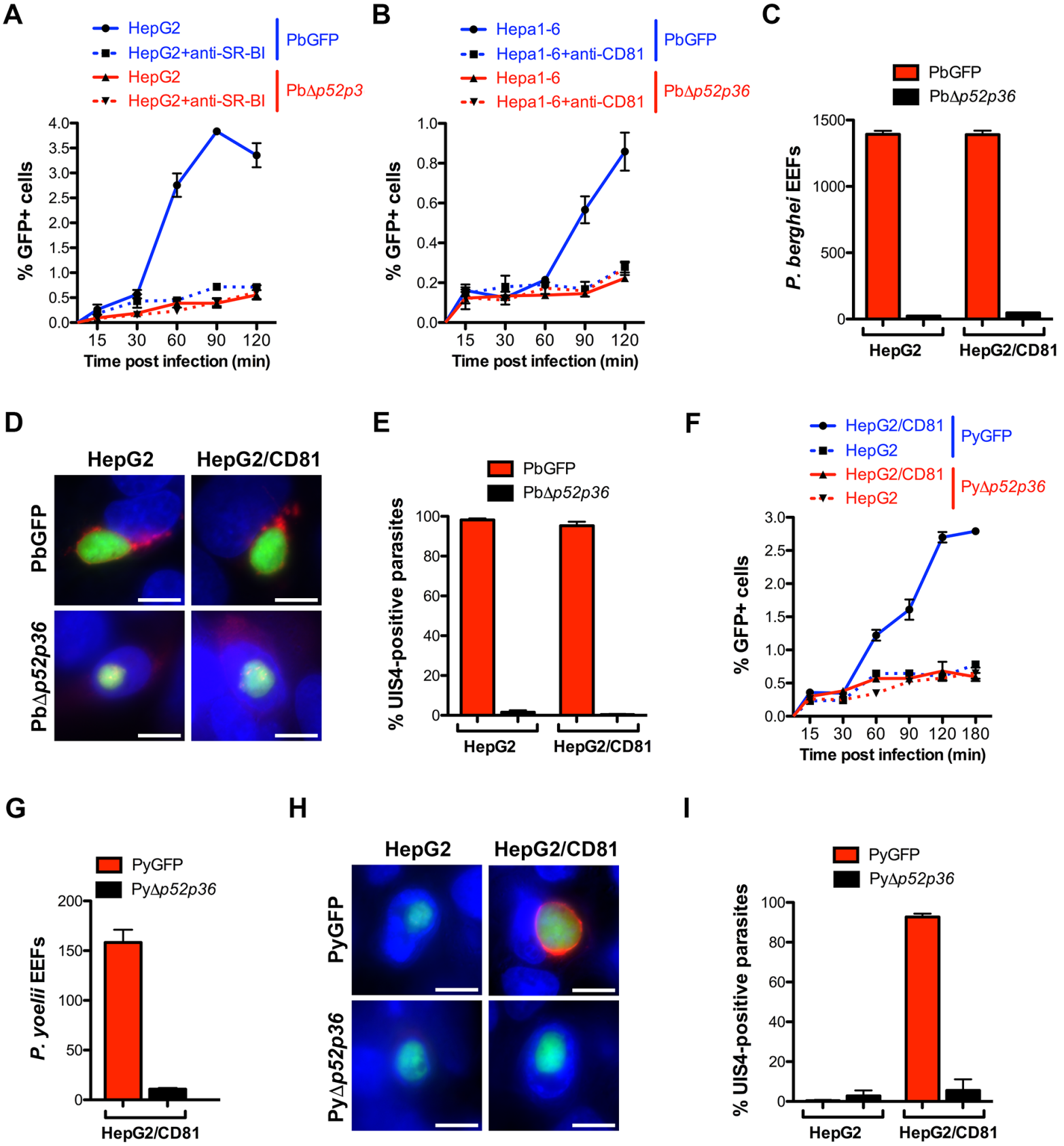
A
HepG2
HepG2+anti-SR-BI
PbGFP
HepG2
HepG2+anti-SR-BI
PbΔp52p3
% GFP+ cells
Time post infection (min)
B
Hepa1-6
Hepa1-6+anti-CD81
PbGFP
Hepa1-6
Hepa1-6+anti-CD81
PbΔp52p36
% GFP+ cells
Time post infection (min)
C
PbGFP
PbΔp52p36
P. berghei EEFs
HepG2
HepG2/CD81
D
HepG2
HepG2/CD81
PbGFP
PbΔp52p36
E
PbGFP
PbΔp52p36
% UIS4-positive parasites
HepG2
HepG2/CD81
F
HepG2/CD81
HepG2
PyGFP
HepG2/CD81
HepG2
PyΔp52p36
% GFP+ cells
Time post infection (min)
G
PyGFP
PyΔp52p36
P. yoelii EEFs
HepG2/CD81
H
HepG2
HepG2/CD81
PyGFP
PyΔp52p36
I
PyGFP
PyΔp52p36
% UIS4-positive parasites
HepG2
HepG2/CD81

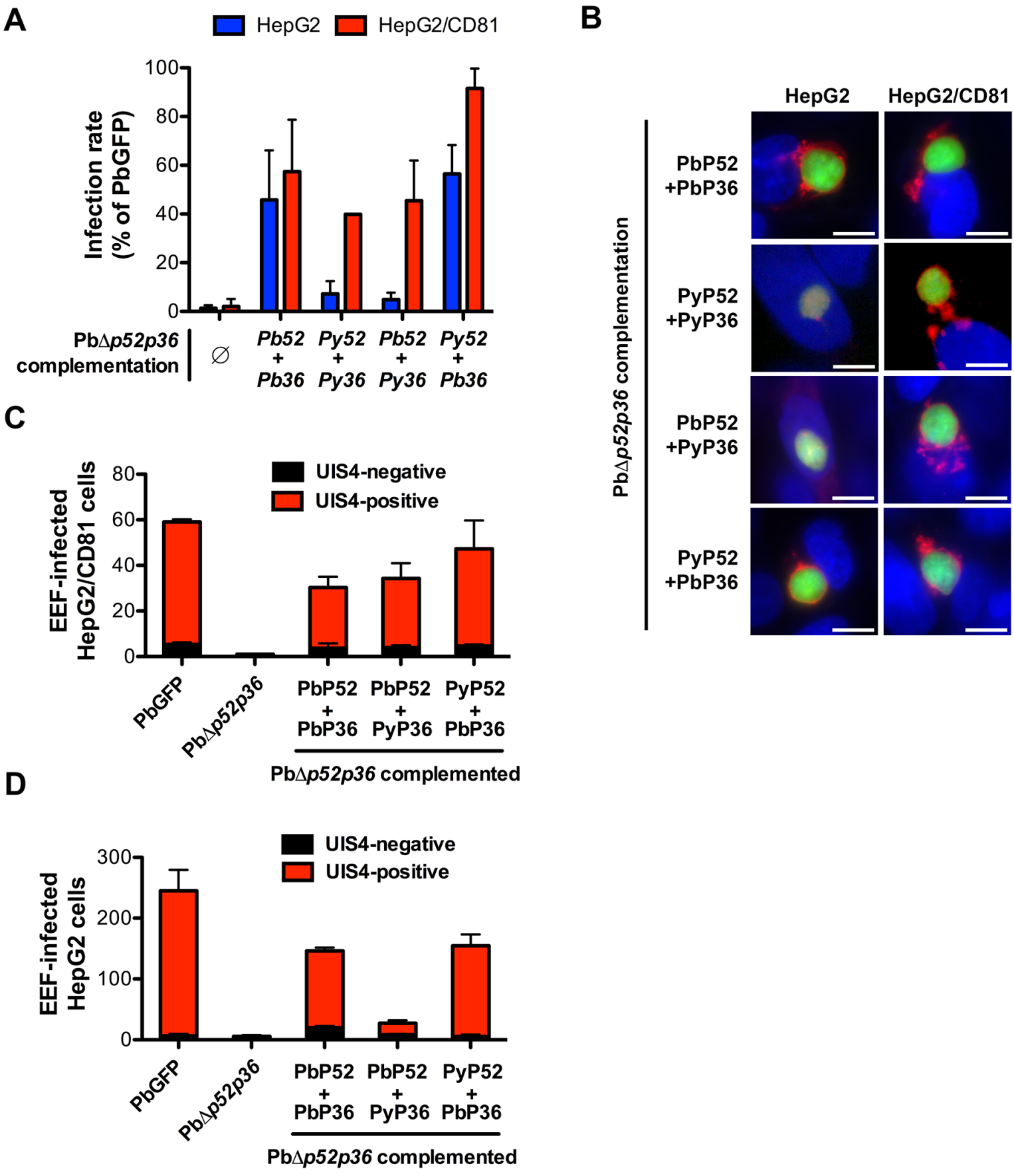
A
HepG2
HepG2/CD81
Infection rate (% of PbGFP)
100
80
60
40
20
0
PbΔp52p36 complementation
∅
Pb52 + Pb36
Py52 + Py36
Pb52 + Py36
Py52 + Pb36
B
HepG2
HepG2/CD81
PbΔp52p36 complementation
PbP52 +PbP36
PyP52 +PyP36
PbP52 +PyP36
PyP52 +PbP36
C
EEF-infected HepG2/CD81 cells
80
60
40
20
0
UIS4-negative
UIS4-positive
PbGFP
PbΔp52p36
PbP52 + PbP36
PbP52 + PyP36
PyP52 + PbP36
PbΔp52p36 complemented
D
EEF-infected HepG2 cells
300
200
100
0
UIS4-negative
UIS4-positive
PbGFP
PbΔp52p36
PbP52 + PbP36
PbP52 + PyP36
PyP52 + PbP36
PbΔp52p36 complemented

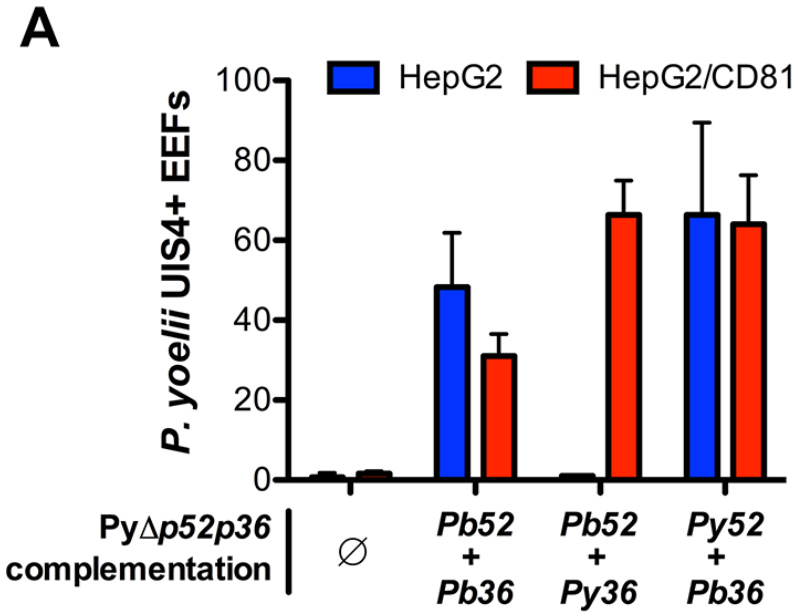
A
HepG2
HepG2/CD81
P. yoelii UIS4+ EEFs
100
80
60
40
20
0
PyΔp52p36 complementation
∅
Pb52 + Pb36
Pb52 + Py36
Py52 + Pb36

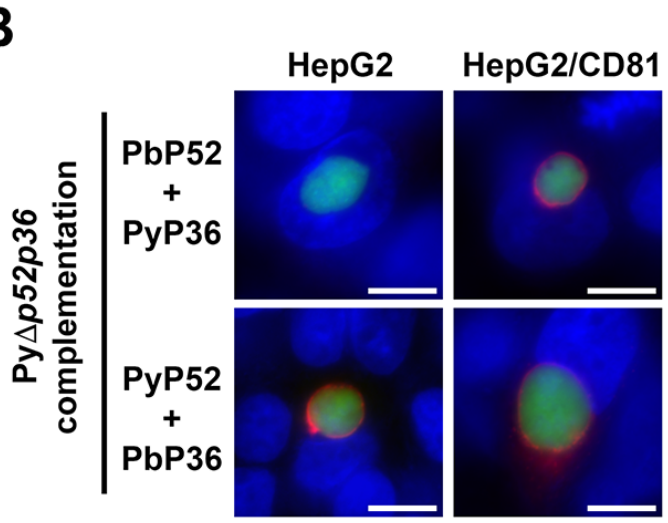
B
HepG2
HepG2/CD81
PyΔp52p36 complementation
PbP52 + PyP36
PyP52 + PbP36

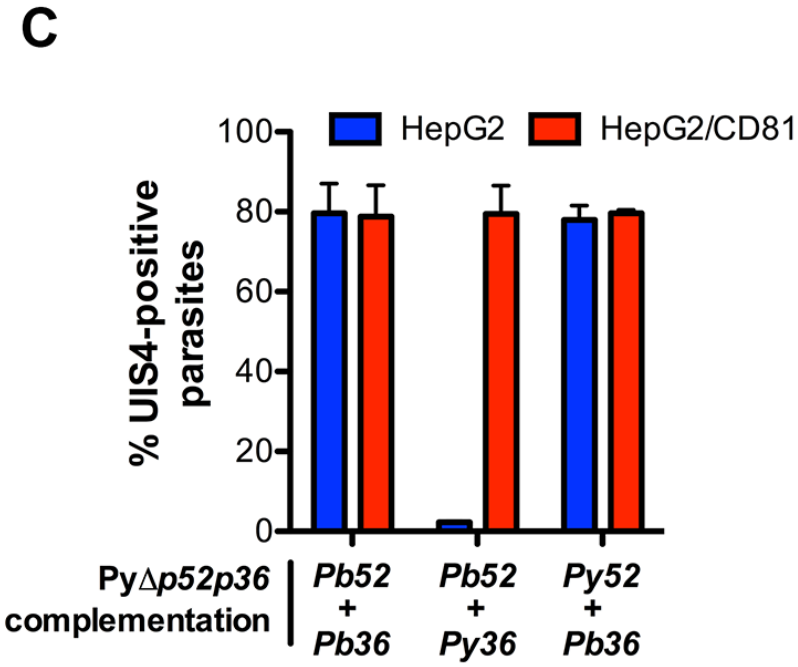
C
HepG2
HepG2/CD81
% UIS4-positive parasites
100
80
60
40
20
0
PyΔp52p36 complementation
Pb52 + Pb36
Pb52 + Py36
Py52 + Pb36

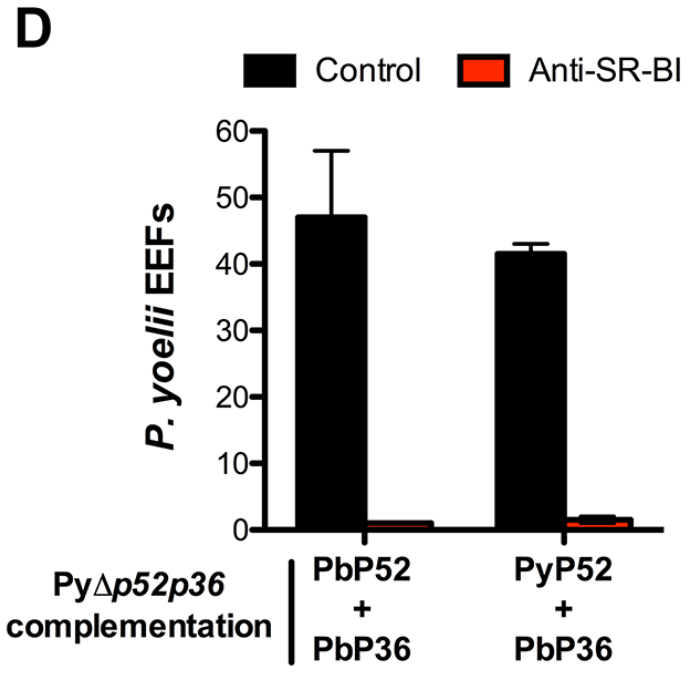
D
Control
Anti-SR-BI
P. yoelii EEFs
60
50
40
30
20
10
0
PyΔp52p36 complementation
PbP52 + PbP36
PyP52 + PbP36

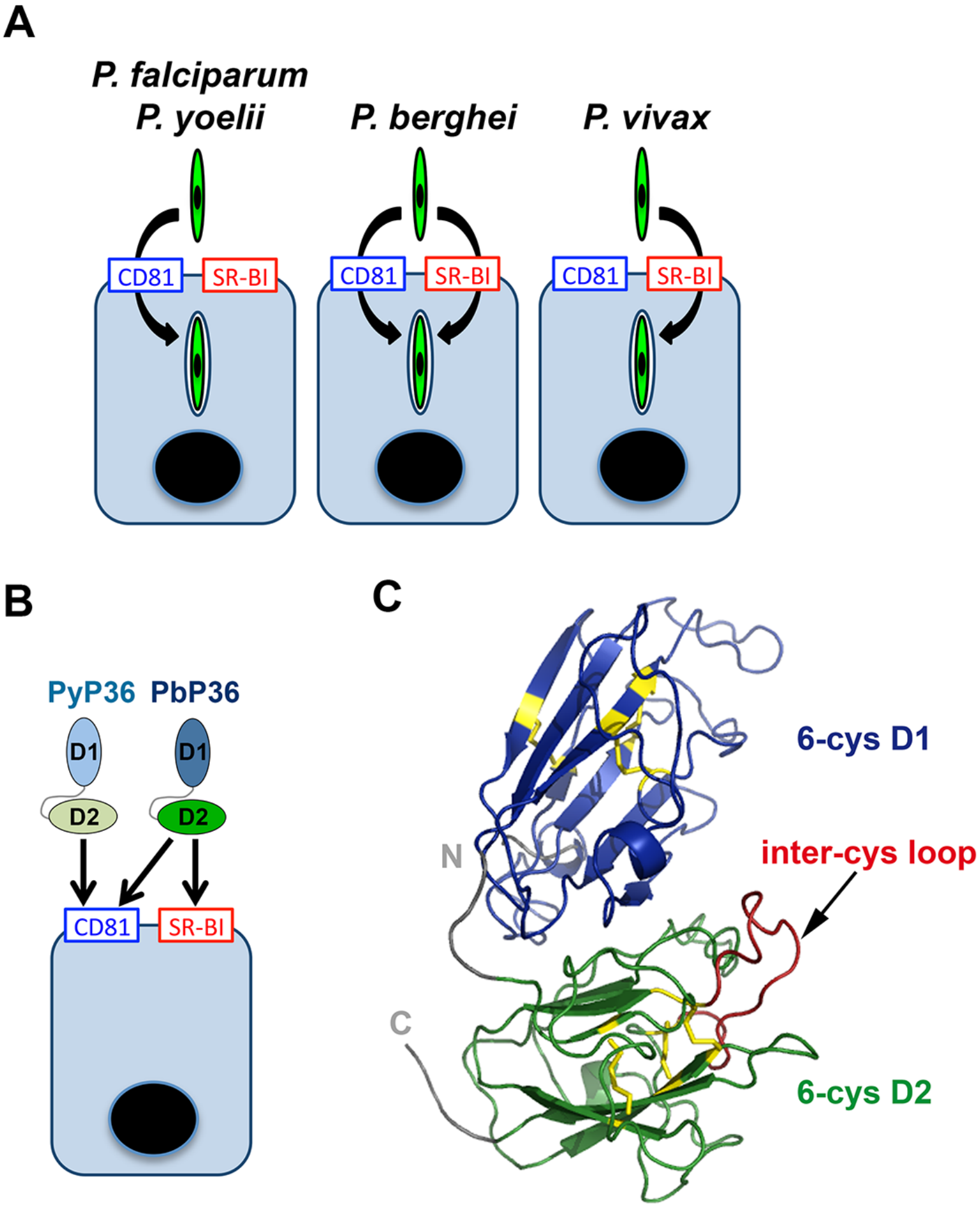
A
P. falciparum
P. yoelii
P. berghei
P. vivax
CD81
SR-BI
CD81
SR-BI
CD81
SR-BI
B
PyP36
PbP36
D1
D1
D2
D2
CD81
SR-BI
C
6-cys D1
inter-cys loop
N
C
6-cys D2

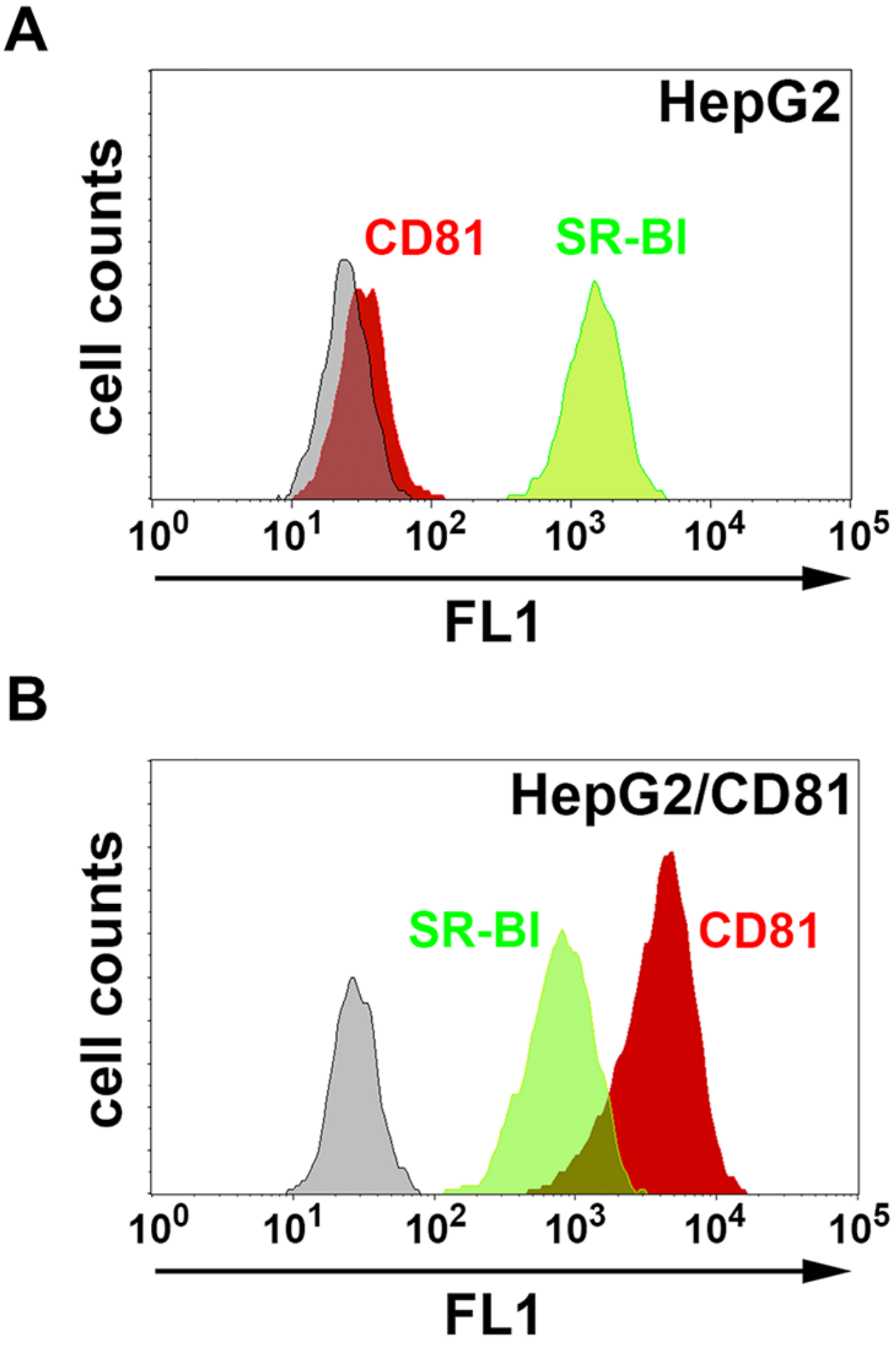
A
HepG2
CD81
SR-BI
cell counts
10^0
10^1
10^2
10^3
10^4
10^5
FL1
B
HepG2/CD81
SR-BI
CD81
cell counts
10^0
10^1
10^2
10^3
10^4
10^5
FL1

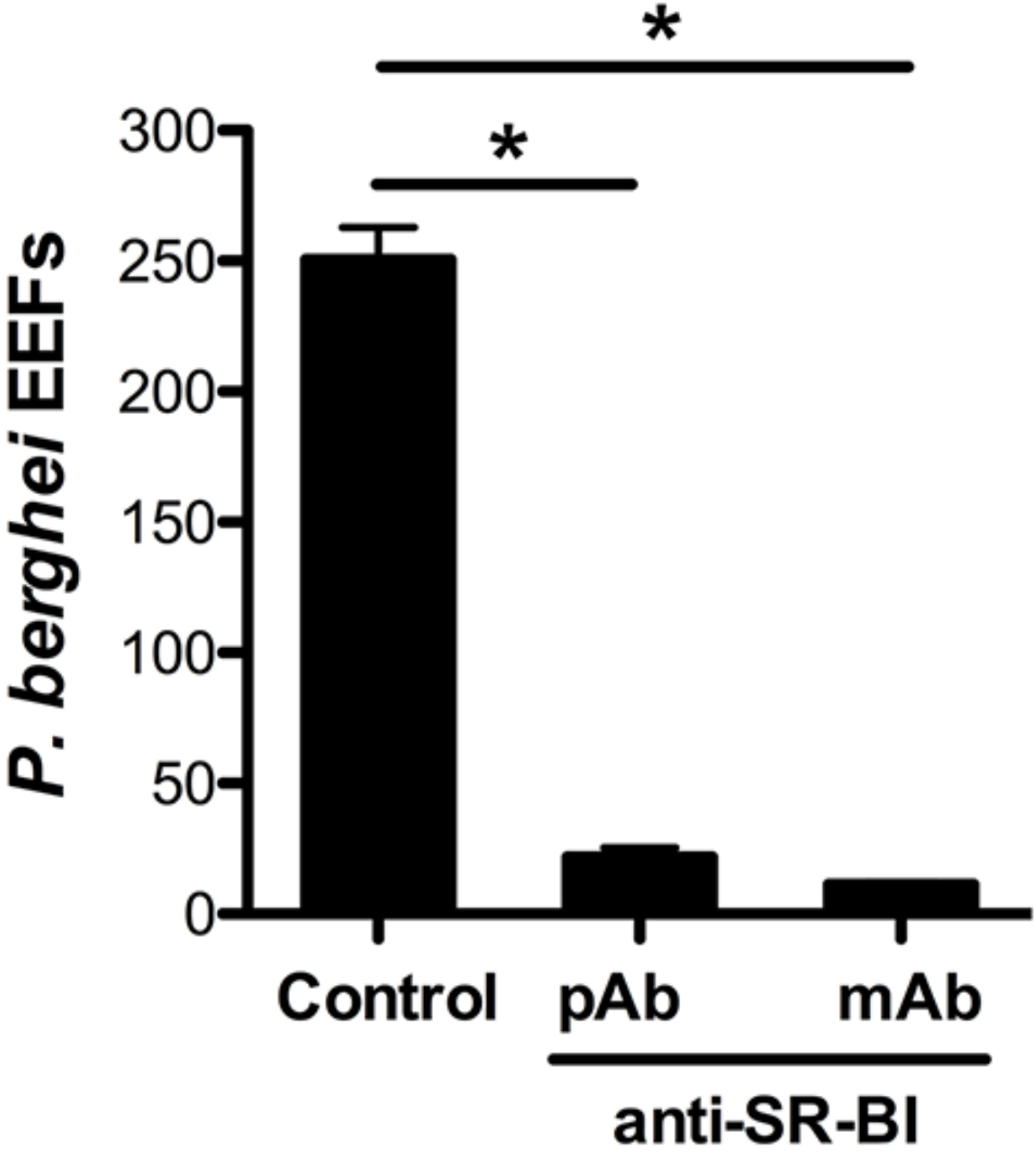
*
*
300
250
200
150
100
50
0
P. berghei EEFs
Control
pAb
mAb
anti-SR-BI

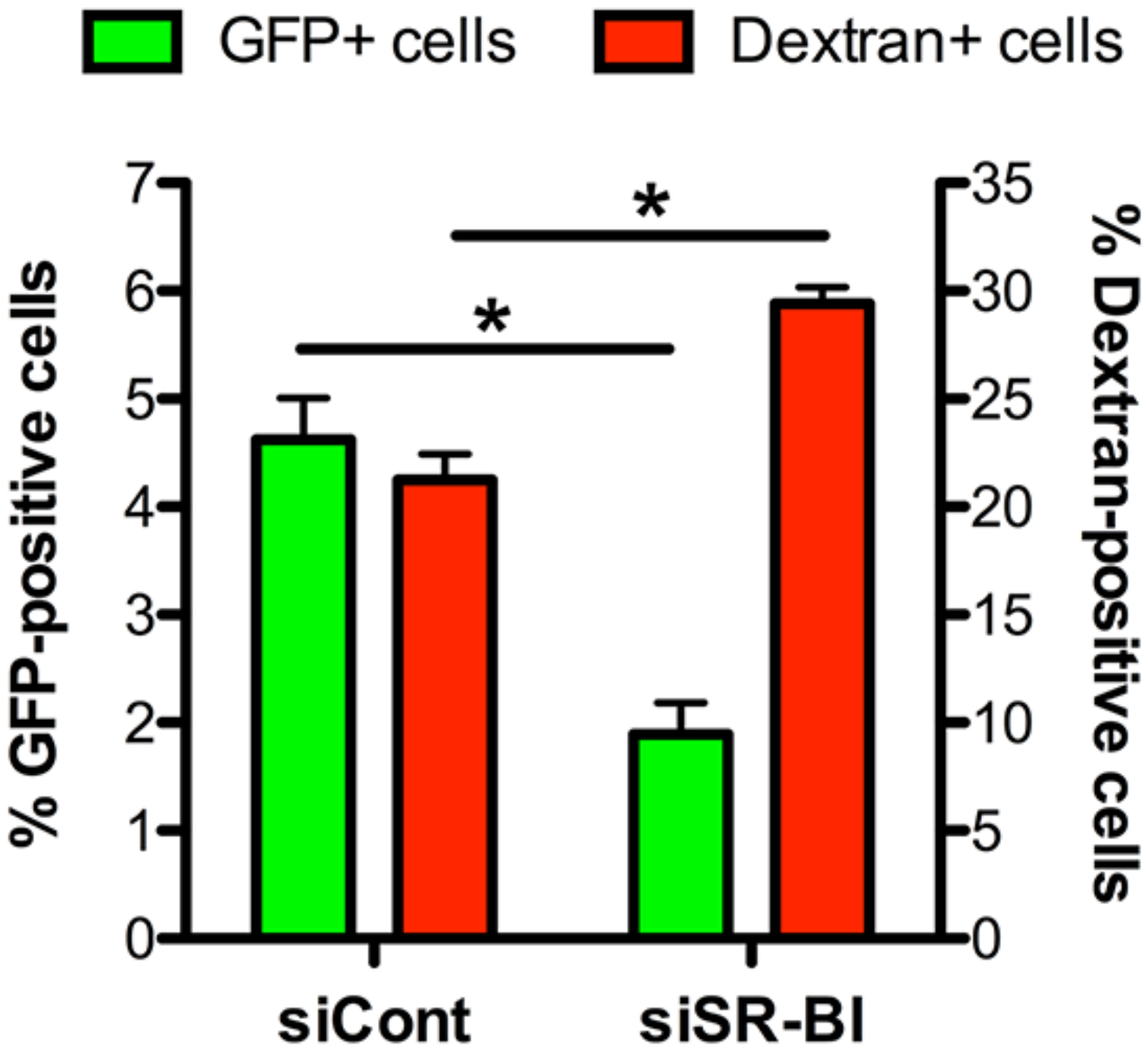
GFP+ cells
Dextran+ cells
% GFP-positive cells
% Dextran-positive cells
0
1
2
3
4
5
6
7
0
5
10
15
20
25
30
35
*
*
siCont
siSR-BI

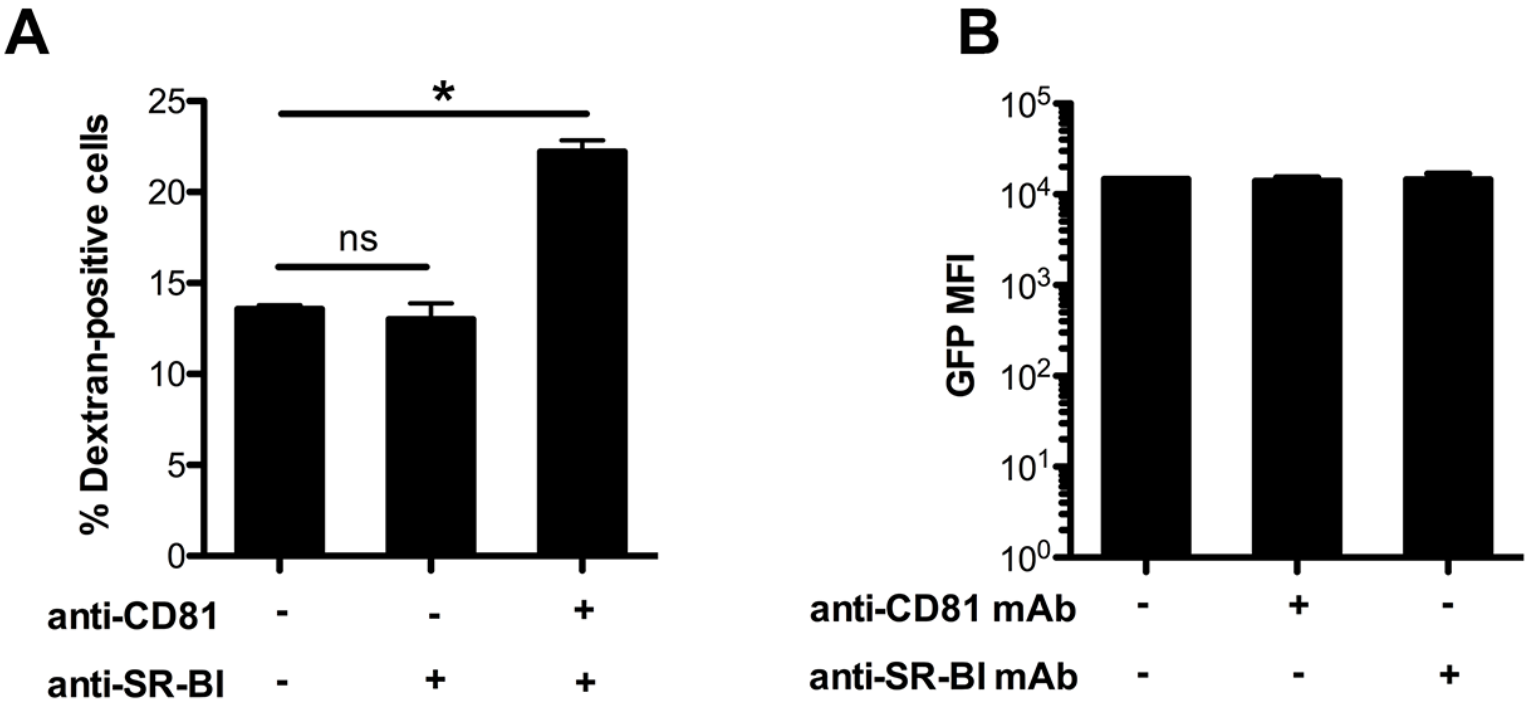
A
% Dextran-positive cells
25
20
15
10
5
0
*
ns
anti-CD81 - - +
anti-SR-BI - + +
B
GFP MFI
10^5
10^4
10^3
10^2
10^1
10^0
anti-CD81 mAb - + -
anti-SR-BI mAb - - +

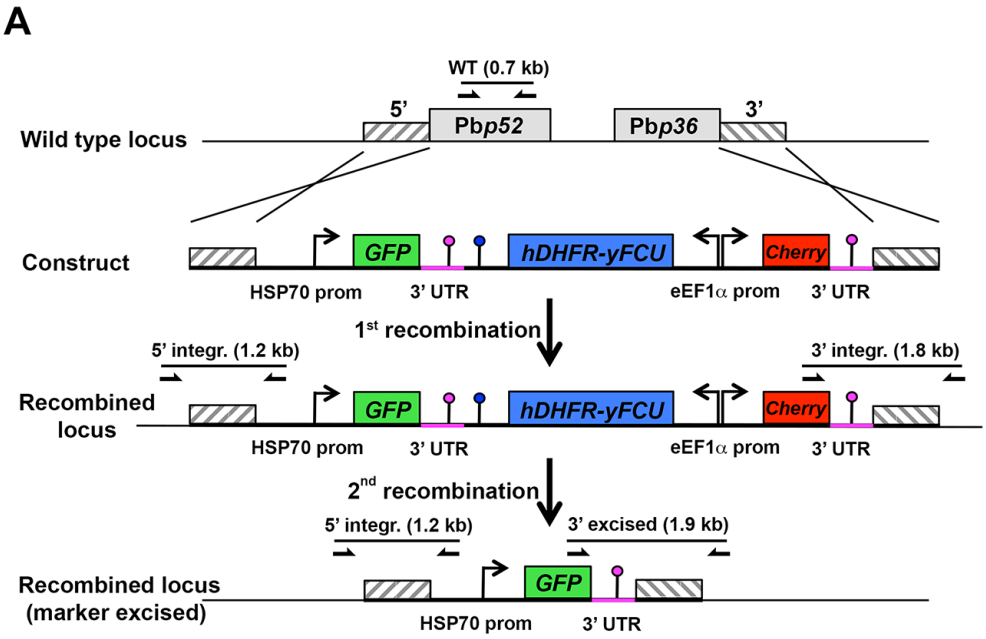
A
WT (0.7 kb)
5'
Pbp52
Pbp36
3'
Wild type locus
Construct
GFP
hDHFR-yFCU
Cherry
HSP70 prom
3' UTR
eEF1α prom
3' UTR
1st recombination
5' integr. (1.2 kb)
3' integr. (1.8 kb)
Recombined locus
2nd recombination
5' integr. (1.2 kb)
3' excised (1.9 kb)
Recombined locus (marker excised)

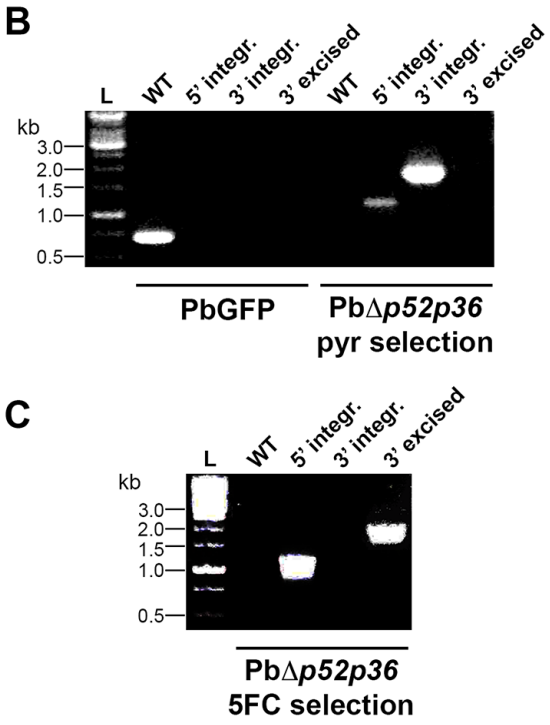
B
L
WT
5' integr.
3' integr.
3' excised
kb
3.0
2.0
1.5
1.0
0.5
PbGFP
PbΔp52p36
pyr selection
C
PbΔp52p36
5FC selection

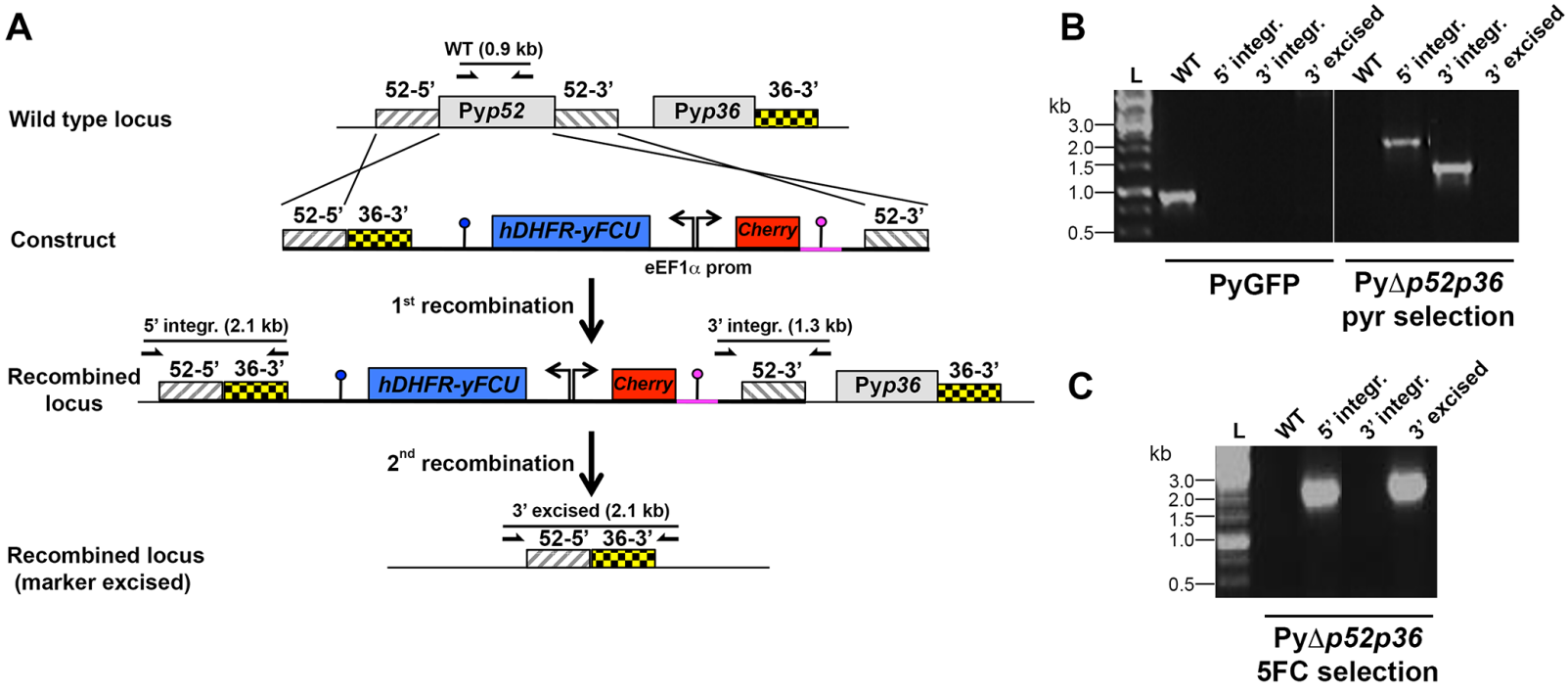
A
WT (0.9 kb)
Wild type locus
52-5'
Py*p52*
52-3'
Py*p36*
36-3'
Construct
52-5'
36-3'
hDHFR-yFCU
Cherry
52-3'
eEF1α prom
1st recombination
5' integr. (2.1 kb)
3' integr. (1.3 kb)
Recombined locus
52-5'
36-3'
hDHFR-yFCU
Cherry
52-3'
Py*p36*
36-3'
2nd recombination
3' excised (2.1 kb)
Recombined locus (marker excised)
52-5'
36-3'
B
L
WT
5' integr.
3' integr.
3' excised
WT
5' integr.
3' integr.
3' excised
kb
3.0
2.0
1.5
1.0
0.5
PyGFP
PyΔ*p52p36* pyr selection
C
L
WT
5' integr.
3' integr.
3' excised
kb
3.0
2.0
1.5
1.0
0.5
PyΔ*p52p36* 5FC selection

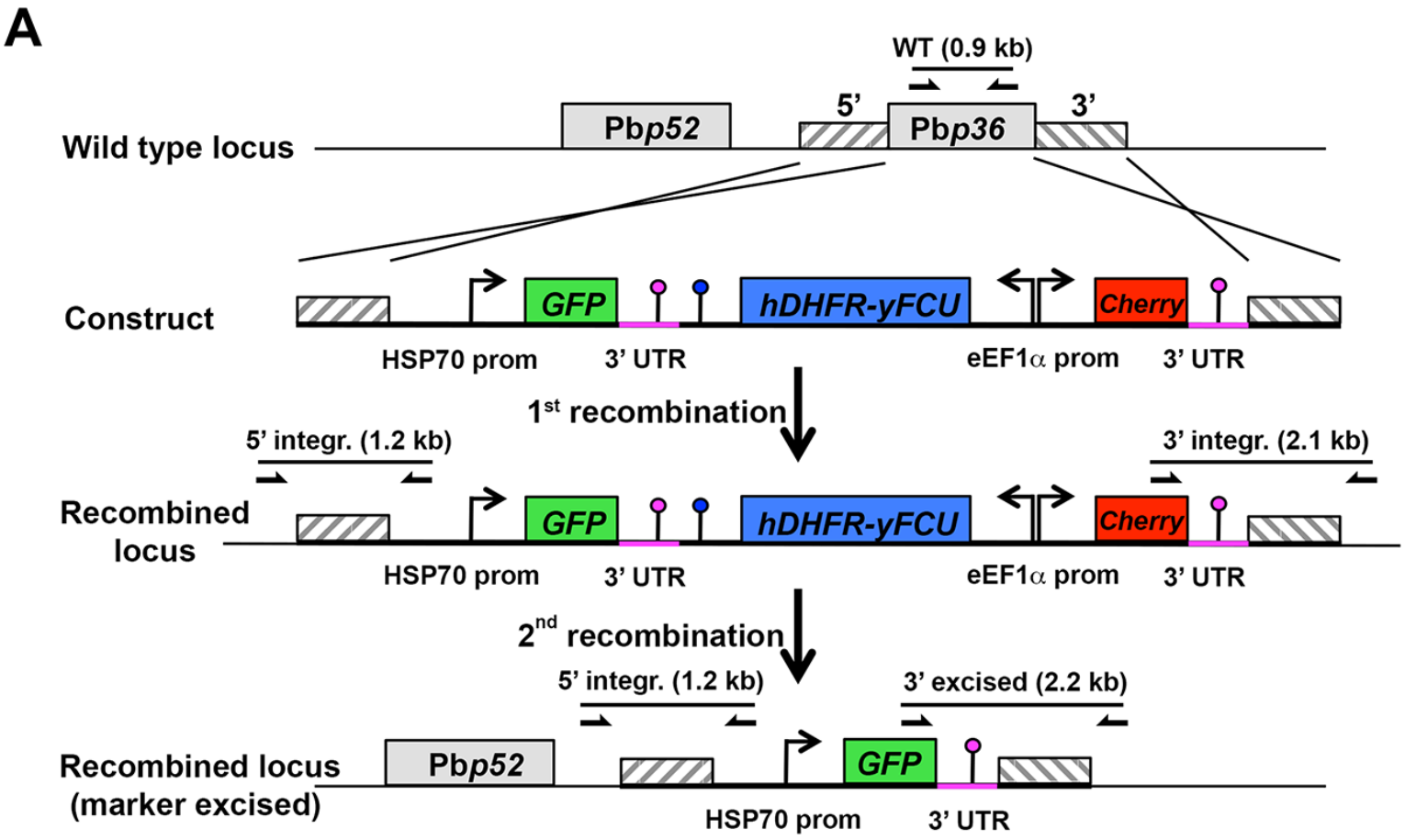
A
WT (0.9 kb)
5'
3'
Wild type locus
Pbp52
Pbp36
Construct
GFP
hDHFR-yFCU
Cherry
HSP70 prom
3' UTR
eEF1α prom
3' UTR
1st recombination
5' integr. (1.2 kb)
3' integr. (2.1 kb)
Recombined locus
2nd recombination
5' integr. (1.2 kb)
3' excised (2.2 kb)
Recombined locus (marker excised)

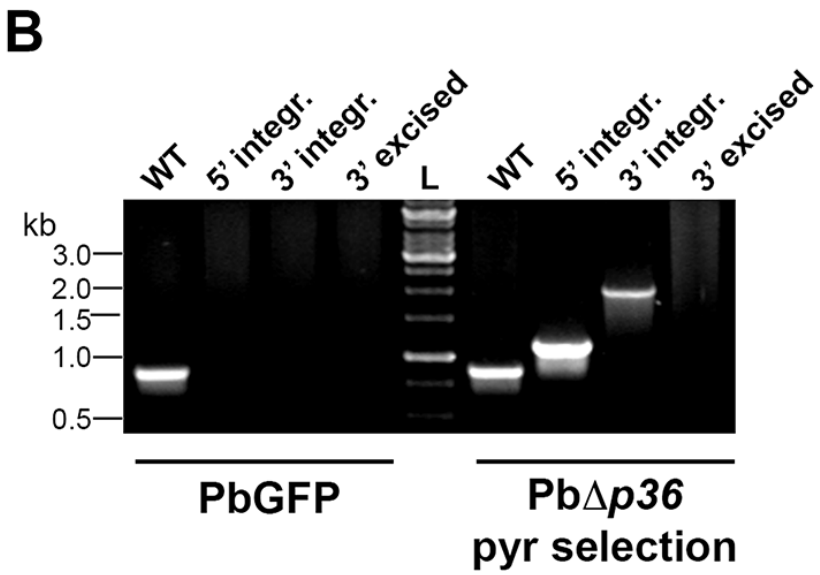
B
WT
5' integr.
3' integr.
3' excised
L
kb
3.0
2.0
1.5
1.0
0.5
PbGFP
PbΔp36
pyr selection

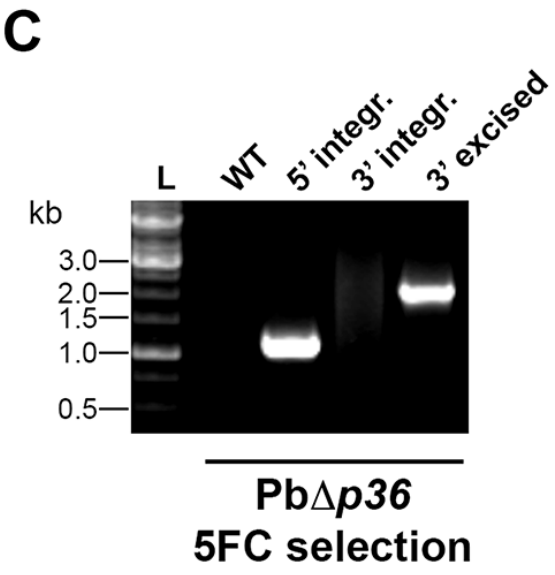
C
L
WT
5' integr.
3' integr.
3' excised
kb
3.0
2.0
1.5
1.0
0.5
PbΔp36
5FC selection

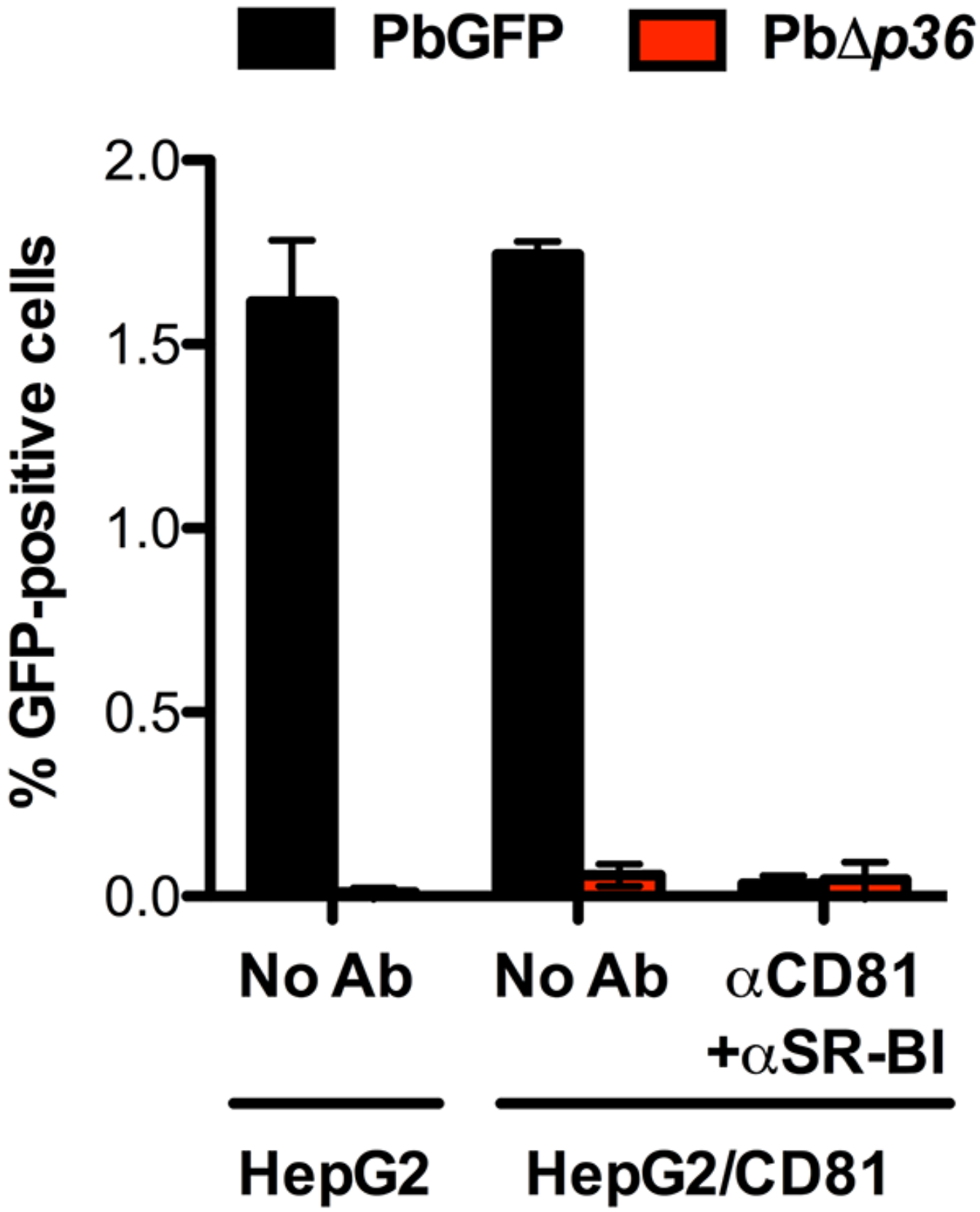
PbGFP
PbΔp36
% GFP-positive cells
2.0
1.5
1.0
0.5
0.0
No Ab
No Ab
αCD81
+αSR-BI
HepG2
HepG2/CD81

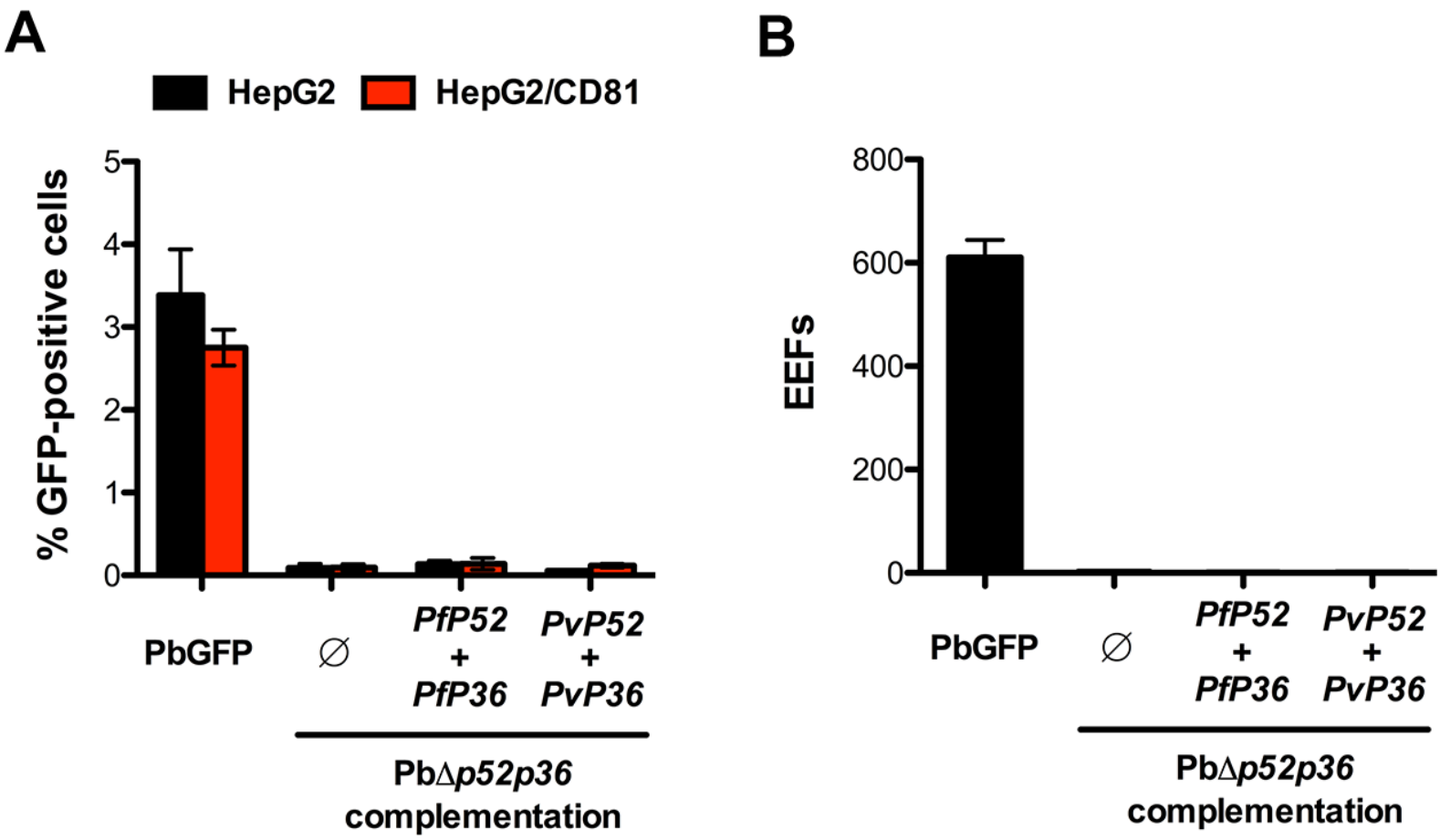
A
HepG2
HepG2/CD81
% GFP-positive cells
5
4
3
2
1
0
PbGFP
∅
PfP52 + PfP36
PvP52 + PvP36
PbΔp52p36 complementation
B
EEFs
800
600
400
200
0
PbGFP
∅
PfP52 + PfP36
PvP52 + PvP36
PbΔp52p36 complementation

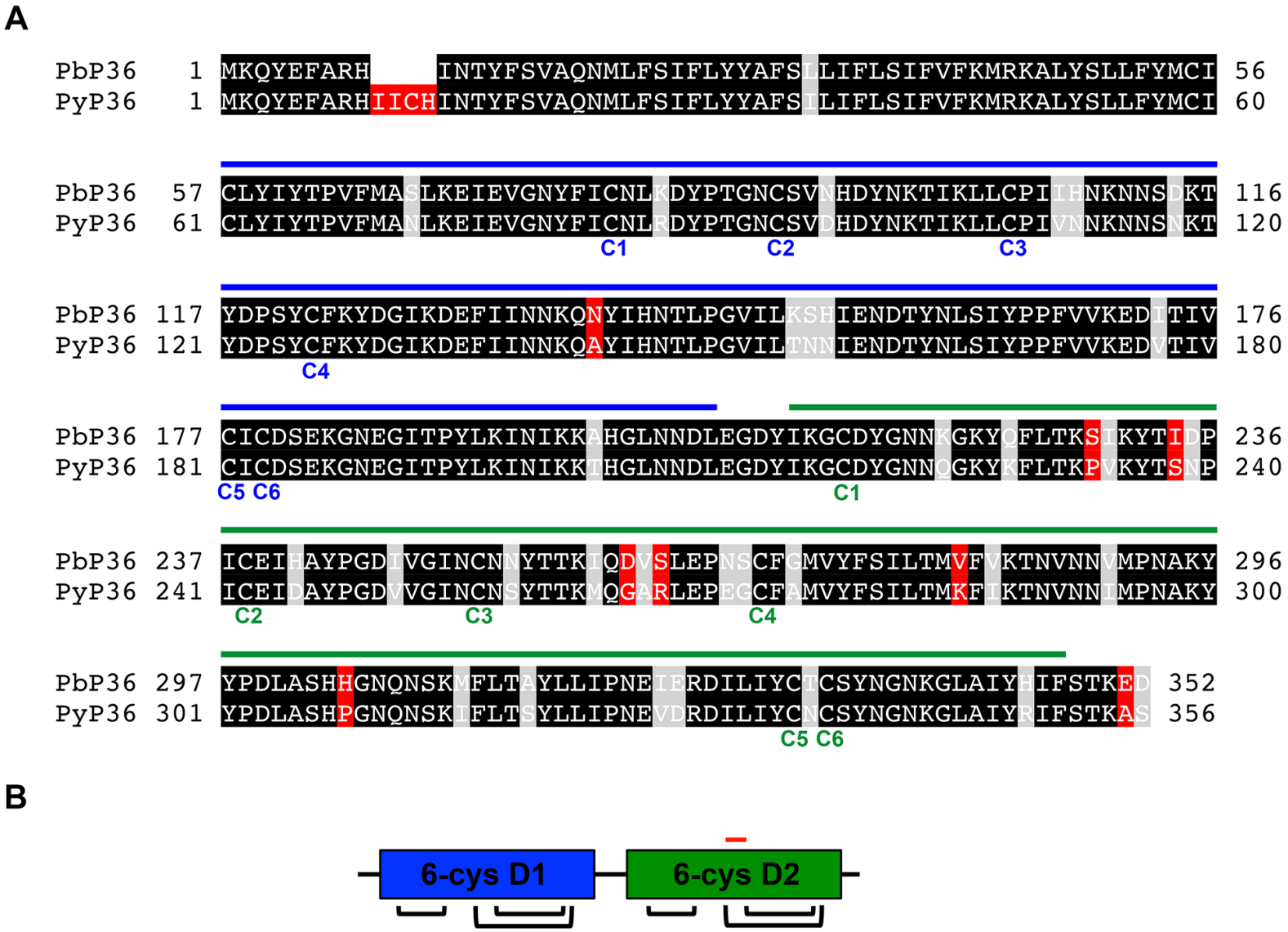
A
PbP36 1 MKQYEFARH INTYFSVAQNMLFSIFLYYAFSLLIFLSIFVFKMRKALYSLLFYMCI 56
PyP36 1 MKQYEFARHIICHINTYFSVAQNMLFSIFLYYAFSLLIFLSIFVFKMRKALYSLLFYMCI 60
PbP36 57 CLYIYTPVFMASLKEIEVGNYFICNLKDYPTGNCSVNHDYNKTIKLLCPIIHNKNNSDKT 116
PyP36 61 CLYIYTPVFMANLKEIEVGNYFICNLRDYPTGNCSVDHDYNKTIKLLCPIVNNKNNSNKT 120
C1
C2
C3
PbP36 117 YDPSYCFKYDGIKDEFIINNKQNYIHNTLPGVILKSHIENDTYNLSIYPPFVVKEDITIV 176
PyP36 121 YDPSYCFKYDGIKDEFIINNKQAYIHNTLPGVILTNNIENDTYNLSIYPPFVVKEDVTIV 180
C4
PbP36 177 CICDSEKGNEGITPYLKINIKKAHGLNNDLEGDYIKGCDYGNNKGKYQFLTKSIKYTIDP 236
PyP36 181 CICDSEKGNEGITPYLKINIKKTHGLNNDLEGDYIKGCDYGNNQGKYKFLTKPVKYTSNP 240
C5 C6
C1
PbP36 237 ICEIHAYPGDIVGINCNNYTTKIQDVSLEPNSCFGMVYFSILTMVFVKTNVNNVMPNAKY 296
PyP36 241 ICEIDAYPGDVVGINCNSYTTKMQGARLEPEGCFAMVYFSILTMKFIKTNVNNLMPNAKY 300
C2
C3
C4
PbP36 297 YPDLASHHGNQNSKMFLTAYLLIPNEIERDILIYCICSYNGNKGLAIYHIFSTKEDD 352
PyP36 301 YPDLASHPGNQNSKIFLTSYLLIPNEVDRDILIYCNCSYNGNKGLAIYRIFSTKASS 356
C5 C6
B
6-cys D1
6-cys D2
C
PfP36 257 CINFEEYTTTTTINNKKKKHQNKNNKNNFDVIQLRPPHC 295
PvP36 245 CINYNEGDL----------QNYEV-KLEPSNC 265
PbP36 252 CNNYTT----------KIQDVS-LEPNSC 269
PyP36 256 CNSYTT----------KMQGAR-LEPEGC 273